

CP-violating Higgs boson mixing in chargino production at the muon collider

OLAF KITTEL

Physikalisches Institut der Universität Bonn, Nussallee 12, D-53115 Bonn, Germany

FEDERICO VON DER PAHLEN

Instituto de Física de Cantabria (CSIC-UC), E-39005 Santander, Spain

Abstract

We study the pair-production of charginos in the CP-violating Minimal Supersymmetric Standard Model at center-of-mass energies around the heavy neutral Higgs boson resonances. If these resonances are nearly degenerate, as it can happen in the Higgs decoupling limit, radiatively induced scalar-pseudoscalar transitions can be strongly enhanced. The resulting mixing in the Higgs sector leads to large CP-violating effects, and a change of their mass spectrum. For longitudinally polarized muon beams, we analyze CP asymmetries which are sensitive to the interference of the two heavy neutral Higgs bosons. We present a detailed numerical analysis of the cross sections, chargino branching ratios, and the CP observables. We obtain sizable CP asymmetries, which would be accessible in future measurements at a muon collider. Especially for intermediate values of the parameter $\tan\beta$, where the largest branching ratios of Higgs bosons into charginos are expected, this process allows to analyze the Higgs sector properties and its interaction to supersymmetric fermions.

1 Introduction

The CP-conserving Minimal Supersymmetric Standard Model (MSSM) contains three neutral Higgs bosons [1–5], the lighter and heavier CP-even scalars h and H , respectively, and the CP-odd pseudoscalar A . In the presence of CP phases, the MSSM Higgs sector is still CP-conserving at Born level. However loop effects, dominantly mediated by third generation squarks, can generate significant CP-violating scalar-pseudoscalar transitions. Thus the neutral CP-odd and CP-even Higgs states mix and form the mass eigenstates H_1, H_2, H_3 , with no definite CP parities [6–14]. A detailed knowledge of their mixing pattern will be crucial for the understanding of the MSSM Higgs sector in the presence of CP-violating phases. The fundamental properties of the Higgs bosons have to be investigated in detail to reveal the mechanism of electroweak symmetry breaking.

The general theoretical formalism for Higgs mixing with CP phases is well developed [10–12, 15]. The results have been implemented in sophisticated public computer programmes [16–18], that allow for numerical higher order calculations of the Higgs masses, widths and couplings. It was shown that CP-violating phases can lead to a lightest Higgs boson with mass of order $M_{H_1} = 45$ GeV [19], which cannot be excluded by measurements at LEP [20]. CP phases can also change the predictions for the Higgs decay widths drastically, see e.g. Ref. [21] for recent calculations for $H_2 \rightarrow H_1 H_1$ at higher order. In general, angular distributions of Higgs decay products will be crucial to probe their CP parities at colliders, for recent studies see, e.g., Ref. [22].

A particularly important feature of the CP-violating Higgs sector is a possible resonance enhanced mixing of the states H and A . It is well known that states with equal conserved quantum numbers can strongly mix if they are nearly degenerate, i.e., if their mass difference is of the order of their widths [8, 13]. This degeneracy occurs naturally in the Higgs decoupling limit of the MSSM, where the lightest Higgs boson has Standard Model-like couplings and decouples from the significantly heavier Higgs bosons [23]. In the decoupling limit, a resonance enhanced mixing of the states H and A can occur, which may result in nearly maximal CP-violating effects [8, 9, 13]. Such effects can only be analyzed thoroughly in processes in which the heavy neutral Higgs bosons can interfere as nearby lying, intermediate resonances [24]. The relative phase information of the two Higgs states would be lost if only their masses, widths and branching ratios are calculated, e.g., by assuming that they are produced as single, on-shell resonances at colliders.

In previous studies of the CP-conserving [25–33] and CP-violating Higgs sector [34–42], it was shown that the interferences of the heavy neutral Higgs bosons can be ideally tested in $\mu^+ \mu^-$ collisions. Since the Higgs bosons are resonantly produced in the s -channel, the muon collider is known to be the ideal machine for measuring the neutral Higgs masses, widths, and couplings with high precision [43–45]. For a systematic classification of CP observables which test the Higgs interference, a preparation of initial muon polarizations *and* the analysis of final fermion polarizations will be crucial. The CP-even and CP-odd contributions of the interfering

Higgs resonances to observables can be ideally studied if the beam polarizations are properly adjusted [29–39]. For example, for final SM fermions $f\bar{f}$, with $f = \tau, b, t$, polarization observables have been classified according to their CP transformation properties [34]. For non-diagonal chargino pair production, the C-odd observables are obtained by antisymmetrizing in the chargino indices of the cross sections, and complete the necessary set of observables [7, 33, 46, 47]. Finally, the well controllable beam energy of the muon collider then allows to study the center-of-mass energy dependence of the observables around the Higgs resonances. This is an advantage over the photon collider, where direct line-shape scans are not possible [48].

In this work, we extend the study of chargino production at the muon collider [33] to the CP-violating case. First results for chargino production in the MSSM with explicit CP violation in the Higgs sector have been reported in Ref. [7]. We classify all CP-even and CP-odd observables for chargino production $\mu^+\mu^- \rightarrow \tilde{\chi}_i^- \tilde{\chi}_j^+$, using longitudinally polarized muon beams. We analyze the longitudinal chargino polarizations by their subsequent leptonic two-body decays $\tilde{\chi}_j^+ \rightarrow \ell^+ \tilde{\nu}_\ell$, with $\ell = e, \mu, \tau$, and the charge conjugated process $\tilde{\chi}_j^- \rightarrow \ell^- \tilde{\nu}_\ell^*$. Asymmetries in the energy distributions of the decay leptons allow us to classify all CP-even and a CP-odd observables for chargino decay, which probe the chargino polarization. Similar asymmetries can be defined for the energy distributions of W bosons, stemming from the decays $\tilde{\chi}_j^\pm \rightarrow W^\pm \tilde{\chi}_k^0$. We find that the muon collider provides the ideal testing ground for phenomenological studies of the Higgs interferences, although it might only be built in the far future. Our analysis gives a deeper understanding of the Higgs mixings, and allows us to test the public codes regarding the relative phase information of the Higgs states in the presence of CP-violating phases.

In Section 2, we give our formalism for chargino production and decay with longitudinally polarized muon beams. In an effective Born-improved approach, we include the leading self-energy corrections into the Higgs couplings. We give analytical formulas for the production and decay cross sections and distributions. We show that also the energy distributions of the chargino decay products depend sensitively on the Higgs interference. In Section 3, we classify the asymmetries of the production cross section and of the energy distributions according to their CP properties. For the production of unequal charginos $\tilde{\chi}_1^\pm \tilde{\chi}_2^\mp$, we also define a new set of C-odd asymmetries. In Section 4, we present a detailed numerical study of the cross sections, chargino branching ratios, and the CP observables. We analyze their dependence on \sqrt{s} , on the CP-violating phase ϕ_A of the common trilinear scalar coupling parameter A , and on the gaugino and higgsino mass parameters μ and M_2 . We complete our analysis by comparing the results with the CP observables obtained in neutralino production [32, 42]. We summarize and conclude in Section 5.

2 Chargino production and decay formalism

We study CP violation in the Higgs sector in pair production of charginos

$$\mu^+ + \mu^- \rightarrow \tilde{\chi}_i^- + \tilde{\chi}_j^+, \quad (1)$$

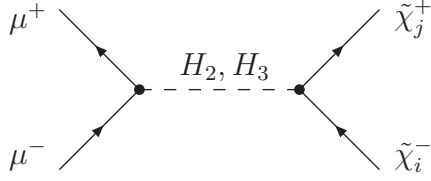


Figure 1: Resonant Higgs exchange in chargino pair production $\mu^+\mu^- \rightarrow \tilde{\chi}_i^-\tilde{\chi}_j^+$.

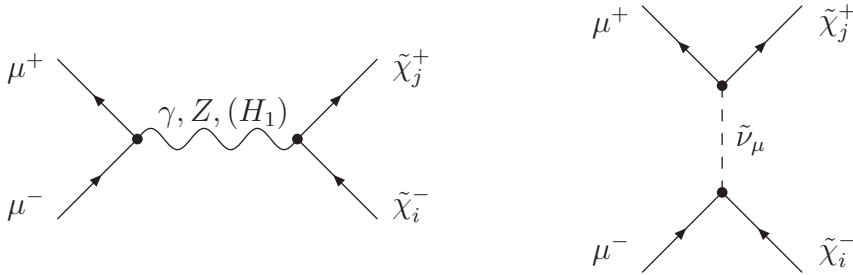


Figure 2: Feynman diagrams for non-resonant chargino production $\mu^+\mu^- \rightarrow \tilde{\chi}_i^-\tilde{\chi}_j^+$

with longitudinally polarized muon beams. We analyze the production of charginos at center-of-mass energies of the nearly mass degenerate heavy neutral Higgs bosons H_2 and H_3 . They will be resonantly produced in the s -channel, see the Feynman diagrams in Fig. 1. The significantly lighter Higgs boson H_1 is also exchanged in the s -channel, however is suppressed far from its resonance. Together with sneutrino exchange $\tilde{\nu}_\mu$ in the t -channel, and Z and γ exchange in the s -channel, they are the non-resonant continuum contributions to chargino production, see the Feynman diagrams in Fig. 2.

To analyze the longitudinal chargino polarization, we consider the subsequent CP-conserving but P-violating leptonic two-body decay of one of the charginos

$$\tilde{\chi}_j^+ \rightarrow \ell^+ + \tilde{\nu}_\ell, \quad (2)$$

and the charge conjugated process $\tilde{\chi}_j^- \rightarrow \ell^- + \tilde{\nu}_\ell^*$. We will focus on the case $\ell = e, \mu$. However our results can be extended to $\ell = \tau$, and for the chargino decay into a W boson

$$\tilde{\chi}_j^\pm \rightarrow W^\pm + \tilde{\chi}_k^0, \quad (3)$$

for which we give the relevant formulas in Appendix D.

2.1 Higgs mixing

CP violation in the MSSM Higgs sector is induced by scalar-pseudoscalar transitions at loop level. The mixing is given by the symmetric and complex Higgs mass

matrix [16]

$$\mathbf{M}(p^2) = \begin{pmatrix} m_h^2 - \hat{\Sigma}_{hh}(p^2) & -\hat{\Sigma}_{hH}(p^2) & -\hat{\Sigma}_{hA}(p^2) \\ -\hat{\Sigma}_{hH}(p^2) & m_H^2 - \hat{\Sigma}_{HH}(p^2) & -\hat{\Sigma}_{HA}(p^2) \\ -\hat{\Sigma}_{hA}(p^2) & -\hat{\Sigma}_{HA}(p^2) & m_A^2 - \hat{\Sigma}_{AA}(p^2) \end{pmatrix} \quad (4)$$

at momentum squared p^2 in the tree-level basis of the CP eigenstates h, H, A . Here $\hat{\Sigma}_{rs}(p^2)$, with $r, s = h, H, A$, are the renormalized self energies of the Higgs bosons at one loop, supplemented with higher-order contributions, see Ref. [16].

The Higgs propagator matrix

$$\Delta(p^2) = -i[p^2 - \mathbf{M}(p^2)]^{-1}, \quad (5)$$

has complex poles at $p^2 = \mathcal{M}_{H_k}^2 = M_{H_k}^2 - iM_{H_k}\Gamma_{H_k}$, $k = 1, 2, 3$, where M_{H_k} and Γ_{H_k} are the mass and width of the Higgs boson mass eigenstate H_k , respectively, with convention $M_{H_1} \leq M_{H_2} \leq M_{H_3}$.

At fixed $p^2 = s$, we may diagonalize the Higgs mass matrix \mathbf{M} , and consequently the propagator Δ , by a complex orthogonal matrix $C = C(s)$,

$$\mathbf{M}_D(s) = C \mathbf{M}(s) C^{-1}, \quad \Delta_D(s) = C \Delta(s) C^{-1}. \quad (6)$$

The diagonal elements of the propagator Δ_D are given in the Breit-Wigner form by

$$[\Delta_D(s)]_{kk} = \frac{-i}{s - [\mathbf{M}_D(s)]_{kk}} \equiv \frac{-i}{s - M_{H_k}'^2 + iM_{H_k}'\Gamma_{H_k}'} \equiv \Delta'(H_k), \quad (7)$$

which defines the s -dependent real parameters M_{H_k}' and Γ_{H_k}' . In the limit $s \rightarrow \mathcal{M}_{H_k}^2$, these parameters are the on-shell mass and decay width of the Higgs boson H_k , $M_{H_k}' \rightarrow M_{H_k}$ and $\Gamma_{H_k}' \rightarrow \Gamma_{H_k}$, respectively. If the s -dependence of the mass matrix \mathbf{M} is weak around the resonance $s \approx M_{H_k}^2$ of a Higgs boson H_k , the kk -element of the propagator can be approximated by

$$\Delta'(H_k) \approx \Delta(H_k) = \frac{-i}{s - M_{H_k}^2 + iM_{H_k}\Gamma_{H_k}}. \quad (8)$$

The approximations $M_{H_k}' \approx M_{H_k}$ and $\Gamma_{H_k}' \approx \Gamma_{H_k}$ hold for instance, if no thresholds open around the Higgs resonance.

In our numerical calculations, we evaluate the mass matrix $\mathbf{M}(p^2)$ and the diagonalization matrix $C(p^2)$ at fixed $p^2 = M_{H_2}^2 \approx M_{H_3}^2$ with the program **FeynHiggs 2.5.1** [16, 17]. We find that the momentum dependence of $\mathbf{M}(p^2)$ is weak around the resonances, and thus $\Delta'(H_k) \approx \Delta(H_k)$ to a very good approximation. For the following discussions, we set $\Delta'(H_k) = \Delta(H_k)$ for simplicity, and drop the prime index of the propagator in our notation.

2.2 Effective Higgs couplings and transition amplitudes

The amplitude for chargino production in muon-antimuon annihilation via Higgs exchange can be written in the general form

$$T^P = \Gamma^{(\chi)} \Delta(s) \Gamma^{(\mu)} \quad (9)$$

$$= \Gamma^{(\chi)} C^{-1} C \Delta(s) C^{-1} C \Gamma^{(\mu)} \quad (10)$$

$$= \Gamma^{(\chi)} C^{-1} \Delta_D(s) C \Gamma^{(\mu)} = \Gamma_{\text{eff}}^{(\chi)} \Delta_D(s) \Gamma_{\text{eff}}^{(\mu)}, \quad (11)$$

where $\Gamma^{(\chi)}$ and $\Gamma^{(\mu)}$ are the one-particle irreducible (1PI) Higgs vertices to charginos and muons, respectively. We have used the basis transformation of the Higgs propagator $\Delta(s)$ at fixed center-of-mass energy s , Eq. (6), which leads to the definition of the effective 1PI vertices $\Gamma_{\text{eff}}^{(\mu)}$ and $\Gamma_{\text{eff}}^{(\chi)}$. The Higgs mixing corrections are thus effectively included via the diagonalization matrix C into the 1PI vertices.

If the Higgs bosons are nearly mass degenerate, the radiative corrections to the propagator matrix are strongly enhanced by the Higgs mixing, and constitute the dominant contributions to the transition amplitude T^P (11). Thus we only include these radiative corrections and neglect specific vertex corrections. The effective Higgs couplings to the initial muons, $c_{L,R}^{H_k\mu\mu}$, and the final charginos, $c_{L,R}^{H_k\chi_i\chi_j}$, are then obtained by transforming the tree level couplings $c_{L,R}^{h_\alpha\mu\mu}$ and $c_{L,R}^{h_\alpha\chi_i\chi_j}$, respectively, with the matrix C , see Eq. (6),

$$c_{L,R}^{H_k\mu\mu} = C_{k\alpha} c_{L,R}^{h_\alpha\mu\mu}, \quad (12)$$

$$c_{L,R}^{H_k\chi_i\chi_j} = \tilde{C}_{k\alpha} c_{L,R}^{h_\alpha\chi_i\chi_j}, \quad h_\alpha = h, H, A. \quad (13)$$

The tree level Higgs couplings are defined and discussed, e.g., in detail in Refs. [3,33]. Note that the final state chargino couplings transform with $\tilde{C} = C^{-1T}$. If the non-physical phases of the Higgs bosons are chosen appropriately, the matrix C can be made complex orthogonal, which implies $\tilde{C} = C$ [49].

With the Born-improved effective couplings of Eqs. (12) and (13), we can write the Higgs exchange amplitude for chargino production

$$\begin{aligned} T^P = \Delta(H_k) & \left[\bar{v}(p_{\mu^+}) \left(c_L^{H_k\mu\mu} P_L + c_R^{H_k\mu\mu} P_R \right) u(p_{\mu^-}) \right] \\ & \times \left[\bar{u}(p_{\chi_j^+}) \left(c_L^{H_k\chi_i\chi_j} P_L + c_R^{H_k\chi_i\chi_j} P_R \right) v(p_{\chi_i^-}) \right] \end{aligned} \quad (14)$$

in its Born-improved form. The amplitudes and Lagrangians for non-resonant γ , Z and $\tilde{\nu}_\mu$ exchange are given in Appendix C, and the Lagrangians for the chargino decays, Eqs. (2) or (3), are given in Appendix D.

2.3 Squared amplitude

In order to calculate the squared amplitude for chargino production (1) and the subsequent decay of chargino $\tilde{\chi}_j^+$, Eqs. (2) or (3), with initial beam polarizations

and complete spin correlations, we use the spin density matrix formalism [50, 51]. Following the detailed steps as given in Appendix A, the squared amplitude in this formalism can be written as

$$|T|^2 = 2|\Delta(\tilde{\chi}_j^+)|^2(PD + \sum_{a=1}^3 \Sigma_P^a \Sigma_D^a), \quad (15)$$

with the propagator $\Delta(\tilde{\chi}_j^+)$ of the decaying chargino, see Eq. (A.7). Here P denotes the unpolarized production of the charginos and D the unpolarized decay. The corresponding polarized terms are Σ_P^a and Σ_D^a , and their product in Eq. (15) describes the chargino spin correlations between production and decay. With our choice of the spin vectors, see Eqs. (A.8) and (A.9), Σ_P^3/P is the longitudinal polarization of $\tilde{\chi}_j^+$, Σ_P^1/P is the transverse polarization in the production plane, and Σ_P^2/P is the polarization perpendicular to the production plane. The terms D and Σ_D^a for chargino decay are given in Appendix D.

The expansion coefficients of the squared chargino production amplitude $|T|^2$ (15) subdivide into contributions from the Higgs resonances (res), the continuum (cont), and the resonance-continuum interference (int), respectively, with

$$P = P_{\text{res}} + P_{\text{cont}}, \quad \Sigma_P^a = \Sigma_{\text{res}}^a + \Sigma_{\text{cont}}^a + \Sigma_{\text{int}}^a, \quad a = 1, 2, 3. \quad (16)$$

The continuum contributions P_{cont} , Σ_{cont}^a are those from the non-resonant γ , Z and $\tilde{\nu}_\mu$ exchange channels, which we give in Appendix C. The contributions from H_1 exchange are suppressed by m_μ^2/s .

The dependence of the resonant contributions P_{res} and Σ_{res}^3 on the longitudinal μ^+ and μ^- beam polarizations \mathcal{P}_+ and \mathcal{P}_- , respectively, is given by¹

$$P_{\text{res}} = (1 + \mathcal{P}_+ \mathcal{P}_-)a_0 + (\mathcal{P}_+ + \mathcal{P}_-)a_1, \quad (17)$$

$$\Sigma_{\text{res}}^3 = (1 + \mathcal{P}_+ \mathcal{P}_-)b_0 + (\mathcal{P}_+ + \mathcal{P}_-)b_1. \quad (18)$$

This expression is useful for analyzing the CP properties of P_{res} and Σ_{res}^3 . The coefficients a_n and b_n , given explicitly in Appendix B, are functions of products of the Higgs couplings to muons and charginos, Eqs. (12) and (13). The coefficients also include the product of Higgs boson propagators, Eq. (7), which strongly depend on the center-of-mass energy, as well as on the CP phases, which enter via the diagonalization matrix C , see the transformation in Eq. (6).

2.4 C and P properties of the Higgs exchange coefficients

We classify the Higgs exchange coefficients a_n and b_n according to their charge (C) and parity (P) properties. Our aim is then to define a complete set of CP-even and CP-odd asymmetries in chargino production and decay, in order to determine the Higgs couplings. The kinematical dependence of the asymmetries can be probed by

¹ The resonant contributions Σ_{res}^1 and Σ_{res}^2 to the transverse polarizations of the chargino vanish for scalar Higgs bosons exchange in the s -channel. Note that there is no interference contribution to the coefficients P and Σ_P^3 .

Table 1: Charge (C) and parity (P) properties of the coefficients a_0^\pm , a_1^\pm , b_0^\pm , and b_1^\pm , see Eqs. (17) and (18), and the corresponding observables for their determination, as defined in Section 3. The four C-odd observables vanish for diagonal chargino production, $i = j$.

coefficient	C	P	CP	observables
a_0^+	+	+	+	σ_{ij}^{C+P+}
a_1^+	+	-	-	\mathcal{A}_{ij}^{C+P-}
a_0^-	-	+	-	\mathcal{A}_{ij}^{C-P+}
a_1^-	-	-	+	\mathcal{A}_{ij}^{C-P-}
b_0^+	+	-	-	$\mathcal{A}_{ij,\ell}^{C+P-}$
b_1^+	+	+	+	$\mathcal{A}_{ij,\ell}^{C+P+}$
b_0^-	-	-	+	$\mathcal{A}_{ij,\ell}^{C-P-}$
b_1^-	-	+	-	$\mathcal{A}_{ij,\ell}^{C-P+}$

line-shape scans. Since a muon collider provides a good beam energy resolution, it will be the ideal tool to analyze the strong \sqrt{s} dependence of the asymmetries.

The factors a_0 and b_1 are P-even, whereas a_1 and b_0 are P-odd. Note that the coefficients a_1 and b_1 only contribute for polarized muon beams. For non-diagonal chargino production, we separate these coefficients into their C-even and C-odd parts, respectively, by symmetric and antisymmetric combinations in the chargino indices,

$$a_n^\pm = \frac{1}{2} [a_n(\tilde{\chi}_i^- \tilde{\chi}_j^+) \pm a_n(\tilde{\chi}_j^- \tilde{\chi}_i^+)], \quad (19)$$

$$b_n^\pm = \frac{1}{2} [b_n(\tilde{\chi}_i^- \tilde{\chi}_j^+) \pm b_n(\tilde{\chi}_j^- \tilde{\chi}_i^+)], \quad n = 0, 1. \quad (20)$$

The coefficients $a_n(\tilde{\chi}_j^- \tilde{\chi}_i^+)$ and $b_n(\tilde{\chi}_j^- \tilde{\chi}_i^+)$ of chargino $\tilde{\chi}_j^-$, for the production of the charge conjugated pair of charginos, $\mu^+ \mu^- \rightarrow \tilde{\chi}_j^- \tilde{\chi}_i^+$, are obtained by interchanging the indices i and j in the formulas of the coefficients defined in Eqs. (B.14)-(B.18), which are defined for $\mu^+ \mu^- \rightarrow \tilde{\chi}_j^+ \tilde{\chi}_i^-$. We summarize the C, P and CP properties of the coefficients, and thus of our observables, in Table 1. Note that, for these observables, CP and $CP\tilde{T}$ are equivalent, since they are built using the longitudinal polarizations only. Here \tilde{T} is the naive time reversal $t \rightarrow -t$, which inverts momenta and spins without exchanging initial and final particles.

2.5 Energy distributions of the chargino decay products

The energy distribution of the lepton or W boson from the chargino decay, Eqs. (2) or (3), respectively, depends on the longitudinal chargino polarization. In the

center-of-mass system, the kinematical limits of the energy of the decay particle $\lambda = e, \mu, \tau, W$ are

$$E_{\lambda}^{\max(\min)} = \hat{E}_{\lambda} \pm \Delta_{\lambda}, \quad (21)$$

which read for the leptonic ($\lambda = \ell$) chargino decays

$$\hat{E}_{\ell} = \frac{E_{\ell}^{\max} + E_{\ell}^{\min}}{2} = \frac{m_{\chi_j^{\pm}}^2 - m_{\tilde{\nu}_{\ell}}^2}{2m_{\chi_j^{\pm}}^2} E_{\chi_j^{\pm}}, \quad (22)$$

$$\Delta_{\ell} = \frac{E_{\ell}^{\max} - E_{\ell}^{\min}}{2} = \frac{m_{\chi_j^{\pm}}^2 - m_{\tilde{\nu}_{\ell}}^2}{2m_{\chi_j^{\pm}}^2} |\vec{p}_{\chi_j^{\pm}}|, \quad \ell = e, \mu, \tau. \quad (23)$$

The energy limits $E_W^{\max(\min)}$ for the W boson are given in Appendix D.

Using the definition of amplitude squared, the cross section, Eqs. (15), and the explicit form of Σ_D^3 (D.50), the energy distribution of the decay particle λ^{\pm} is [32,33]

$$\frac{d\sigma_{ij,\lambda^{\pm}}}{dE_{\lambda}} = \frac{\sigma_{ij,\lambda}}{2\Delta_{\lambda}} \left[1 + \eta_{\lambda^{\pm}} \frac{\bar{\Sigma}_P^3}{\bar{P}} \frac{(E_{\lambda} - \hat{E}_{\lambda})}{\Delta_{\lambda}} \right], \quad (24)$$

The integrated cross section for chargino production and decay is denoted by $\sigma_{ij,\lambda^{\pm}}$, e.g. for the decay $\tilde{\chi}_j^+ \rightarrow \ell^+ \tilde{\nu}_{\ell}$ it is, using the narrow width approximation for the propagator of the decaying chargino,

$$\sigma_{ij,\ell} = \sigma_{ij} \times \text{BR}(\tilde{\chi}_j^+ \rightarrow \ell^+ \tilde{\nu}_{\ell}), \quad (25)$$

where σ_{ij} is the cross section for $\tilde{\chi}_i^- \tilde{\chi}_j^+$ production. Explicit expressions for the cross sections σ_{ij} , $\sigma_{ij,\ell}$, and $\sigma_{ij,W}$ are given in Appendix E. The factor $\eta_{\lambda^{\pm}}$ is a measure of parity violation in the chargino decay. It is maximal $\eta_{e^{\pm}}, \eta_{\mu^{\pm}} = \pm 1$ for the decay into leptons of the first two generations, while for the decay $\tilde{\chi}_j^{\pm} \rightarrow \tau^{\pm} \tilde{\nu}_{\tau}^{(*)}$, it is generally smaller $|\eta_{\tau^{\pm}}| < 1$. In Appendix D, we give explicit expressions of the factors $\eta_{\tau^{\pm}}$, as well as $\eta_{W^{\pm}}$ for the decay $\tilde{\chi}_j^{\pm} \rightarrow W^{\pm} \tilde{\chi}_k^0$.

Further, from Eq. (24), we see that the energy distribution is proportional to the chargino polarization $\bar{\Sigma}_P^3/\bar{P}$. The coefficients $\bar{\Sigma}_P^3$ and \bar{P} are averaged over the chargino production solid angle

$$\bar{\Sigma}_P^3 = \frac{1}{4\pi} \int \Sigma_P^3 d\Omega_{\chi_j^{\pm}} = \Sigma_{\text{res}}^3 + \bar{\Sigma}_{\text{cont}}^3, \quad \bar{P} = \frac{1}{4\pi} \int P d\Omega_{\chi_j^{\pm}} = P_{\text{res}} + \bar{P}_{\text{cont}}, \quad (26)$$

denoted by a bar in our notation. Note that the resonant contributions from Higgs exchange are isotropic $\bar{\Sigma}_{\text{res}}^3 = \Sigma_{\text{res}}^3$, $\bar{P}_{\text{res}} = P_{\text{res}}$.

In Fig. 3, we show the energy distributions (24) of the leptons ℓ^{\pm} from the decays $\tilde{\chi}_j^+ \rightarrow \ell^+ \tilde{\nu}_{\ell}$ and $\tilde{\chi}_j^- \rightarrow \ell^- \tilde{\nu}_{\ell}^*$, for $\ell = e$ or μ . The cutoffs in the energy distributions of the leptons ℓ^+ and ℓ^- correspond to their kinematical limits, as given in Eq. (21). We see the linear dependence of the distributions on the lepton energy. Their slope is proportional to the longitudinal chargino polarization $\bar{\Sigma}_P^3/\bar{P}$, see Eq. (24). Note that the energy distribution might be difficult to measure for a small chargino-sneutrino mass difference, since the energy span of the observed lepton is proportional to the difference of their squared masses, see Eq. (23).

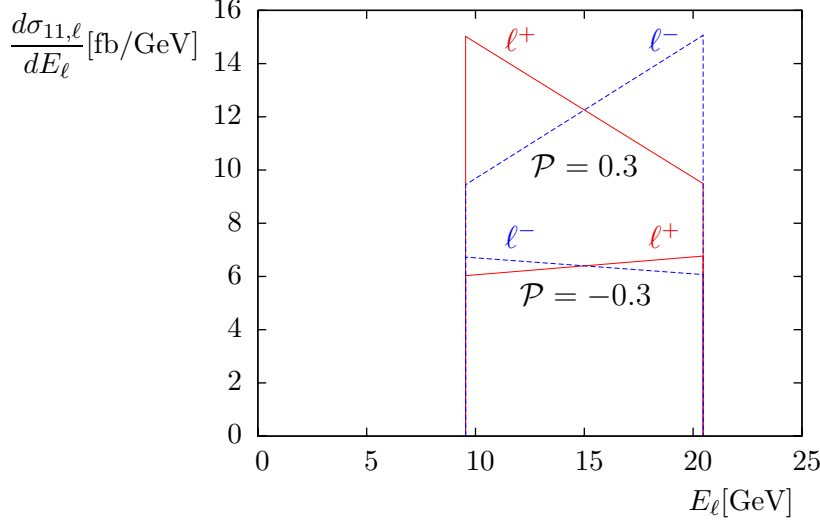


Figure 3: Energy distributions of the leptons ℓ^\pm for chargino production $\mu^+\mu^- \rightarrow \tilde{\chi}_1^+\tilde{\chi}_1^-$ and decay $\tilde{\chi}_1^+ \rightarrow \ell^+\tilde{\nu}_\ell$ (solid, red), and $\tilde{\chi}_1^- \rightarrow \ell^-\tilde{\nu}_\ell^*$ (dashed, blue) for $\ell = e$ or μ , at $\sqrt{s} = (M_{H_2} + M_{H_3})/2$ with longitudinal beam polarizations $\mathcal{P}_- = \mathcal{P}_+ \equiv \mathcal{P} = +0.3$ and $\mathcal{P} = -0.3$. The MSSM parameters are given in Tables 2 and 3. The shown distributions have asymmetries (for $\mathcal{P} = 0.3$) $\mathcal{A}_{11,\ell^+} = -11.3\%$ and $\mathcal{A}_{11,\ell^-} = 11.45\%$, (for $\mathcal{P} = -0.3$) $\mathcal{A}_{11,\ell^+} = 2.9\%$ and $\mathcal{A}_{11,\ell^-} = -2.6\%$, see Eq. (36).

3 Chargino production and decay observables

For chargino pair production $\mu^+\mu^- \rightarrow \tilde{\chi}_i^-\tilde{\chi}_j^+$, we have expanded the resonant contributions P_{res} (17) and Σ_{res}^3 (18) to the spin density matrix elements in terms of the longitudinal muon beam polarizations \mathcal{P}_\pm . We have classified the coefficients a_0^\pm , a_1^\pm , b_0^\pm , and b_1^\pm according to their charge (C) and parity (P) transformation properties, see Table 1. In order to determine the coefficients a_0^\pm and a_1^\pm , we define one production cross section observable and three asymmetries of the chargino production cross section in the following section. To determine the coefficients b_0^\pm and b_1^\pm of the chargino polarization, the chargino decays have to be taken into account. We therefore define an additional set of four asymmetries of the energy distributions of the decay particle. In Table 1, we also list the observables which we define in the following sections. Non-diagonal chargino production $i \neq j$ leads to the four C-odd observables, which vanish trivially for diagonal chargino production $i = j$.

3.1 Asymmetries of the chargino production cross section

In order to classify the CP observables in chargino production, we define in a first step the symmetric and antisymmetric combinations

$$\sigma_{ij}^{\text{C}+} = \frac{1}{2}(\sigma_{ij} + \sigma_{ji}), \quad \sigma_{ij}^{\text{C}-} = \frac{1}{2}(\sigma_{ij} - \sigma_{ji}), \quad (27)$$

of the production cross section σ_{ij} (E.68). The combinations are relevant for non-diagonal chargino production, with $i \neq j$. The indices C_+ and C_- indicate the even and odd parity under charge (C) conjugation, respectively. In a second step, we obtain observables which have a definite parity (P) by symmetrizing and antisymmetrizing in the common muon beam polarizations $\mathcal{P}_+ = \mathcal{P}_- \equiv \mathcal{P}$.

The C- and P-even observable is obtained by symmetrizing $\sigma_{ij}^{\text{C}+}$ (27) in \mathcal{P}

$$\sigma_{ij}^{\text{C}+\text{P}+} = \frac{1}{2} \left[\sigma_{ij}^{\text{C}+}(\mathcal{P}) + \sigma_{ij}^{\text{C}+}(-\mathcal{P}) \right]. \quad (28)$$

Inserting the explicit form of σ_{ij} (E.68) and P_{res} (17) the coefficient a_0^+ can be determined,

$$\sigma_{ij}^{\text{C}+\text{P}+} = \frac{\sqrt{\lambda_{ij}}}{8\pi s^2} \left[(1 + \mathcal{P}^2) a_0^+ + \bar{P}_{\text{cont}} \right], \quad (29)$$

if the continuum contributions \bar{P}_{cont} (16) can be subtracted, e.g, through a side-band analysis, where the cross section is extrapolated around the resonances [28], and/or by chargino cross section measurements at the International Linear Collider (ILC) [54, 55].

The two CP-odd asymmetries are obtained by [7, 45]

$$\mathcal{A}_{ij}^{\text{C}+\text{P}-} = \frac{\sigma_{ij}^{\text{C}+}(\mathcal{P}) - \sigma_{ij}^{\text{C}+}(-\mathcal{P})}{\sigma_{ij}^{\text{C}+}(\mathcal{P}) + \sigma_{ij}^{\text{C}+}(-\mathcal{P})}, \quad (30)$$

and

$$\mathcal{A}_{ij}^{\text{C}-\text{P}+} = \frac{\sigma_{ij}^{\text{C}-}(\mathcal{P}) + \sigma_{ij}^{\text{C}-}(-\mathcal{P})}{\sigma_{ij}^{\text{C}+}(\mathcal{P}) + \sigma_{ij}^{\text{C}+}(-\mathcal{P})}. \quad (31)$$

The CP-even asymmetry is [7]

$$\mathcal{A}_{ij}^{\text{C}-\text{P}-} = \frac{\sigma_{ij}^{\text{C}-}(\mathcal{P}) - \sigma_{ij}^{\text{C}-}(-\mathcal{P})}{\sigma_{ij}^{\text{C}+}(\mathcal{P}) + \sigma_{ij}^{\text{C}+}(-\mathcal{P})}. \quad (32)$$

Using the definitions of the chargino production cross section σ_{ij} (E.68), and of the coefficient P (17), we obtain

$$\mathcal{A}_{ij}^{\text{C}\pm\text{P}-} = \frac{2\mathcal{P}a_1^\pm}{(1 + \mathcal{P}^2)a_0^+ + \bar{P}_{\text{cont}}}. \quad (33)$$

These asymmetries thus allow to determine a_1^\pm . The coefficient a_0^- can be obtained from

$$\mathcal{A}_{ij}^{\text{C}-\text{P}+} = \frac{(1 + \mathcal{P}^2)a_0^-}{(1 + \mathcal{P}^2)a_0^+ + \bar{P}_{\text{cont}}}. \quad (34)$$

Note that the continuum contributions \bar{P}_{cont} are P-even, $P_{\text{cont}}(\mathcal{P}) = P_{\text{cont}}(-\mathcal{P})$, and C-even, $P_{\text{cont}}(\tilde{\chi}_i^- \tilde{\chi}_j^+) = P_{\text{cont}}(\tilde{\chi}_i^+ \tilde{\chi}_j^-)$, and thus cancel in the numerator of the P-odd and C-odd asymmetries $\mathcal{A}_{ij}^{\text{C}\pm\text{P}-}$ (33) and $\mathcal{A}_{ij}^{\text{C}-\text{P}+}$ (34), respectively.

The maximum absolute values of the P-odd asymmetries depends on the beam polarization \mathcal{P}

$$\mathcal{A}_{ij(\text{max})}^{\text{C}\pm\text{P}-} = \frac{2\mathcal{P}}{1 + \mathcal{P}^2}, \quad (35)$$

which follows from Eq. (34) for vanishing continuum contributions $\bar{P}_{\text{cont}} = 0$. The P-even asymmetry $\mathcal{A}_{ij}^{\text{C-P}+}$ can be as large as 100%.

The CP-odd asymmetries $\mathcal{A}_{ij}^{\text{C+P-}}$ and $\mathcal{A}_{ij}^{\text{C-P+}}$ vanish in the case of CP conservation, and are sensitive to the CP phases of the Higgs boson couplings to the charginos and to the muons. The CP-odd asymmetry $\mathcal{A}_{ij}^{\text{C+P-}}$ is CP \tilde{T} -odd, with \tilde{T} the naive time reversal $t \rightarrow -t$, which inverts momenta and spins without exchanging initial and final particles. Thus the asymmetry is due to the interference of CP phases with absorptive phases from the transition amplitudes. The absorptive phases are also called strong phases, and can originate from intermediate particles in the Higgs self energies which go on-shell. The asymmetry $\mathcal{A}_{ij}^{\text{C+P-}}$ is therefore sensitive to the CP phases of the Higgs boson couplings, as well as to the phases of the Higgs propagators.

In the Higgs decoupling limit [23], the heavy neutral Higgs bosons are nearly mass-degenerate. Thus a mixing of the CP-even and CP-odd Higgs states H and A can be resonantly enhanced, and large CP-violating Higgs couplings can be obtained [8,9]. In addition, if the Higgs bosons are nearly mass-degenerate, CP phases in the Higgs sector lead to a larger splitting of the mass eigenstates H_2 and H_3 . This, in general, tends to increase the phase between the Higgs propagators, giving rise to larger absorptive phases in the transition amplitudes. On the contrary, the observables $\sigma_{ij}^{\text{C+P+}}$ (28) and $\mathcal{A}_{ij}^{\text{C-P-}}$ (32), being CP-even, will be reduced in general in the presence of CP-violating phases.

3.2 Asymmetries of the lepton energy distribution

The longitudinal chargino polarization is also sensitive to the Higgs interference in the production $\mu^+\mu^- \rightarrow \tilde{\chi}_i^\mp \tilde{\chi}_j^\pm$, and yields additional information on the Higgs couplings. The chargino $\tilde{\chi}_j^\pm$ polarization can be analyzed by the subsequent decays $\tilde{\chi}_j^\pm \rightarrow \ell^\pm \tilde{\nu}_\ell^{(*)}$, with $\ell = e, \mu, \tau$, and $\tilde{\chi}_j^\pm \rightarrow W^\pm \tilde{\chi}_k^0$. In Subsection 2.5, we have shown that the slope of the energy distribution of the decay particle $\lambda = \ell, W$, is proportional to the averaged longitudinal chargino polarization $\bar{\Sigma}_P^3/\bar{P}$, see Eq. (24). The polarization can be determined by the energy distribution asymmetry [33]

$$\begin{aligned} \mathcal{A}_{ij,\lambda^\pm} &= \frac{\Delta\sigma_{ij,\lambda^\pm}}{\sigma_{ij,\lambda^\pm}} = \frac{1}{2}\eta_{\lambda^\pm} \frac{\bar{\Sigma}_P^3}{\bar{P}} \\ &= \frac{1}{2}\eta_{\lambda^\pm} \frac{(1 + \mathcal{P}_+\mathcal{P}_-)b_0 + (\mathcal{P}_+ + \mathcal{P}_-)b_1 + \bar{\Sigma}_{\text{cont}}^3}{(1 + \mathcal{P}_+\mathcal{P}_-)a_0 + (\mathcal{P}_+ + \mathcal{P}_-)a_1 + \bar{P}_{\text{cont}}}, \end{aligned} \quad (36)$$

with

$$\Delta\sigma_{ij,\lambda^\pm} = \sigma_{ij,\lambda^\pm}(E_\lambda > \hat{E}_\lambda) - \sigma_{ij,\lambda^\pm}(E_\lambda < \hat{E}_\lambda), \quad (37)$$

and $\lambda = e, \mu, \tau, W$. Here we have used the explicit formula of the energy distribution of the decay particle $\lambda^\pm = \ell^\pm, W^\pm$ (24).

An example of the energy distribution and the corresponding asymmetries $\mathcal{A}_{ij,\lambda^\pm}$ for the leptonic decay $\lambda = e, \mu$, for equal muon beam polarizations $\mathcal{P}_+ = \mathcal{P}_- \equiv \mathcal{P}$,

is given in Fig. 3. The area under each graph equals the corresponding cross section of production and decay, $\sigma_{11,\ell^\pm} = \sigma_{11} \times \text{BR}(\tilde{\chi}_1^\pm \rightarrow \ell^\pm \tilde{\nu}_\ell^{(*)})$, see Eq. (25). Here σ_{11} is larger for $\mathcal{P} > 0$ than for $\mathcal{P} < 0$, since the P-odd asymmetry $\mathcal{A}_{11}^{\text{C+P-}}$ (30) is positive. The slope of the curves is proportional to the averaged longitudinal chargino polarization $\bar{\Sigma}_P^3$, and to the decay factor η_{ℓ^\pm} , with $\eta_{\ell^+} = -\eta_{\ell^-} = 1$. Thus the slope of the energy distribution of ℓ^+ has the opposite sign than that of ℓ^- , each for $\mathcal{P} > 0$ and $\mathcal{P} < 0$ separately. However, the moduli of the slopes are not the same for the two leptons for fixed \mathcal{P} , which can be seen in the different absolute values of the asymmetries, e.g., $\mathcal{A}_{11,\ell^+} = -11.3\%$ and $\mathcal{A}_{11,\ell^-} = 11.45\%$ for $\mathcal{P} = +0.3$. The difference of the absolute values is due to the small continuum contributions, which change sign, depending on the chargino charge, i.e., $\bar{\Sigma}_{\text{cont}}(\tilde{\chi}_1^+) = -\bar{\Sigma}_{\text{cont}}(\tilde{\chi}_1^-)$.

The average chargino polarization depends on the continuum contributions $\bar{\Sigma}_{\text{cont}}^3$, and is also proportional to b_0 and b_1 , see Eq. (36). In order to separate these coefficients into their C-even and -odd parts b_n^+ , b_n^- , respectively, we define the four generalized decay asymmetries of the energy distribution [7],

$$\mathcal{A}_{ij,\lambda}^{\text{C}\pm\text{P}+} = \frac{\Delta\sigma_{ij,\lambda^+}(\mathcal{P}) - \Delta\sigma_{ij,\lambda^+}(-\mathcal{P}) \mp [\Delta\sigma_{ij,\lambda^-}(\mathcal{P}) - \Delta\sigma_{ij,\lambda^-}(-\mathcal{P})]}{\sigma_{ij,\lambda^+}(\mathcal{P}) + \sigma_{ij,\lambda^+}(-\mathcal{P}) + \sigma_{ij,\lambda^-}(\mathcal{P}) + \sigma_{ij,\lambda^-}(-\mathcal{P})} \quad (38)$$

$$= \eta_{\lambda^+} \frac{\mathcal{P} b_1^\pm}{(1 + \mathcal{P}^2) a_0^+ + \bar{P}_{\text{cont}}}, \quad (39)$$

$$\mathcal{A}_{ij,\lambda}^{\text{C+P-}} = \frac{\Delta\sigma_{ij,\lambda^+}(\mathcal{P}) + \Delta\sigma_{ij,\lambda^+}(-\mathcal{P}) - [\Delta\sigma_{ij,\lambda^-}(\mathcal{P}) + \Delta\sigma_{ij,\lambda^-}(-\mathcal{P})]}{\sigma_{ij,\lambda^+}(\mathcal{P}) + \sigma_{ij,\lambda^+}(-\mathcal{P}) + \sigma_{ij,\lambda^-}(\mathcal{P}) + \sigma_{ij,\lambda^-}(-\mathcal{P})} \quad (40)$$

$$= \frac{1}{2} \eta_{\lambda^+} \frac{(1 + \mathcal{P}^2) b_0^+}{(1 + \mathcal{P}^2) a_0^+ + \bar{P}_{\text{cont}}}, \quad (41)$$

$$\mathcal{A}_{ij,\lambda}^{\text{C-P-}} = \frac{\Delta\sigma_{ij,\lambda^+}(\mathcal{P}) + \Delta\sigma_{ij,\lambda^+}(-\mathcal{P}) + \Delta\sigma_{ij,\lambda^-}(\mathcal{P}) + \Delta\sigma_{ij,\lambda^-}(-\mathcal{P})}{\sigma_{ij,\lambda^+}(\mathcal{P}) + \sigma_{ij,\lambda^+}(-\mathcal{P}) + \sigma_{ij,\lambda^-}(\mathcal{P}) + \sigma_{ij,\lambda^-}(-\mathcal{P})} \quad (42)$$

$$= \frac{1}{2} \eta_{\lambda^+} \frac{(1 + \mathcal{P}^2) b_0^- + \bar{\Sigma}_{\text{cont}}^3}{(1 + \mathcal{P}^2) a_0^+ + \bar{P}_{\text{cont}}}, \quad (43)$$

for equal muon beam polarizations $\mathcal{P}_+ = \mathcal{P}_- \equiv \mathcal{P}$. Note that the continuum contributions $\bar{\Sigma}_{\text{cont}}^3$ of the chargino $\tilde{\chi}_j^\pm$ polarization are C-odd, $\bar{\Sigma}_{\text{cont}}^3(\tilde{\chi}_i^- \tilde{\chi}_j^+) = -\bar{\Sigma}_{\text{cont}}^3(\tilde{\chi}_i^+ \tilde{\chi}_j^-)$, and P-even, $\bar{\Sigma}_{\text{cont}}^3(\mathcal{P}) = \bar{\Sigma}_{\text{cont}}^3(-\mathcal{P})$, and thus cancel (only) in the numerator of the C-even and/or P-even asymmetries $\mathcal{A}_{ij,\lambda}^{\text{C}\pm\text{P}+}$ (39) and $\mathcal{A}_{ij,\lambda}^{\text{C+P-}}$ (41), respectively. The asymmetries for the decay into a τ or W boson, $\tilde{\chi}_j^\pm \rightarrow \tau^\pm \tilde{\nu}_\tau^{(*)}$, and $\tilde{\chi}_j^\pm \rightarrow W^\pm \tilde{\chi}_k^0$, respectively, are generally smaller than those for the decays into an electron or muon, due to $|\eta_{\tau^\pm}|, |\eta_{W^\pm}| \leq |\eta_{e^\pm}| = |\eta_{\mu^\pm}| = 1$, see Eqs. (D.63) and (D.62).

The CP-even asymmetry $\mathcal{A}_{ij,\lambda}^{\text{C+P}+}$ (38) is due to the correlation between the longitudinal polarizations of the initial muons and final charginos. Large values of $\mathcal{A}_{ij,\lambda}^{\text{C+P}+}$, and also of $\mathcal{A}_{ij,\lambda}^{\text{C-P-}}$ (42), can be obtained when both Higgs resonances are

nearly degenerate, and if their amplitudes are of the same magnitude. However, a scalar-pseudoscalar mixing in the presence of CP phases will in general increase the mass splitting of the Higgs bosons, and the reduced overlap of the Higgs resonances also reduces the CP-even asymmetry $\mathcal{A}_{ij,\lambda}^{\text{C+P+}}$.

The CP-odd asymmetries $\mathcal{A}_{ij,\lambda}^{\text{C-P+}}$ (38) and $\mathcal{A}_{ij,\lambda}^{\text{C+P-}}$ (40) are sensitive to CP-violating phases and thus vanish for CP-conserving Higgs couplings. Similarly to the CP-odd polarization asymmetry $\mathcal{A}_{ij}^{\text{C+P-}}$ (30) for chargino production, the decay asymmetry $\mathcal{A}_{ij,\lambda}^{\text{C+P-}}$ is approximately maximal if the Higgs mixing is resonantly enhanced. As pointed out earlier, this can happen naturally in the Higgs decoupling limit.

Finally we count the total number of observables which are available in chargino production and decay with longitudinally polarized beams. There are two production and two decay asymmetries/observables, each for $\tilde{\chi}_1^+ \tilde{\chi}_1^-$ and $\tilde{\chi}_2^+ \tilde{\chi}_2^-$ production and decay. Note that the C-odd observables vanish for diagonal chargino production. For $\tilde{\chi}_1^\pm \tilde{\chi}_2^\mp$ production, there are four production observables and four decay observables for the decay of chargino $\tilde{\chi}_1^\pm$, as well as additional four decay observables for the decay of $\tilde{\chi}_2^\pm$. These 20 observables can be used to determine the Higgs couplings in chargino production, see also Table 1.

4 Numerical results

We analyze numerically the CP-even and CP-odd asymmetries for chargino production, $\mu^+ \mu^- \rightarrow \tilde{\chi}_1^+ \tilde{\chi}_1^-$, and $\mu^+ \mu^- \rightarrow \tilde{\chi}_1^\pm \tilde{\chi}_2^\mp$. For the chargino decays, $\tilde{\chi}_{1,2}^\pm \rightarrow \ell^\pm \tilde{\nu}_\ell^{(*)}$, we study the CP-even and CP-odd decay asymmetries of the leptonic energy distributions, which allow to probe the longitudinal chargino polarizations. The feasibility of measuring the asymmetries depends also on the chargino production cross section and decay branching ratios, which we discuss in detail. We will identify regions of the parameter space where a resonant enhanced mixing of the Higgs bosons will lead to nearly maximal CP-violating effects.

We induce CP violation in the Higgs sector by a non-vanishing phase ϕ_A of the common trilinear scalar coupling parameter $A_t = A_b = A_\tau \equiv |A| \exp(i\phi_A)$ for the third generation fermions. This assignment is also compatible with the bounds on CP-violating phases from experiments on electric dipole moments (EDMs) [56–59]. For simplicity we keep the gaugino mass parameters M_1 , M_3 , and the Higgs mass parameter μ real. For the calculation of the Higgs masses, widths and couplings, we use the program **FeynHiggs 2.5.1** [16, 17], see also [42]. We fix $\tan \beta = 10$, since the Higgs boson decays into charginos are most relevant for intermediate values of $\tan \beta$. Smaller values of $\tan \beta$ favor the $t\bar{t}$ decay channel, while larger values enhance decays into $b\bar{b}$ and $\tau\bar{\tau}$. For the branching ratios and width of the decaying chargino, we include the two-body decays [53]

$$\begin{aligned} \tilde{\chi}_{1,2}^\pm &\rightarrow W^\pm + \tilde{\chi}_k^0, e^\pm + \tilde{\nu}_e, \mu^\pm + \tilde{\nu}_\mu, \tau^\pm + \tilde{\nu}_\tau, \nu_e + \tilde{e}_L^\pm, \nu_\mu + \tilde{\mu}_L^\pm, \nu_\tau + \tilde{\tau}_{1,2}^\pm, \\ \tilde{\chi}_2^\pm &\rightarrow Z^0 + \tilde{\chi}_1^\pm, H_1^0 + \tilde{\chi}_1^\pm. \end{aligned} \quad (44)$$

Table 2: SUSY parameters for the benchmark scenario $\text{CP}\chi$. The slepton masses are parametrized by m_0 and M_2 , the squark masses by M_{SUSY} .

$M_{H^\pm} = 500 \text{ GeV}$	$\tan \beta = 10$	$ A = 1 \text{ TeV}$	$\phi_A = 0.2\pi$
$M_{\text{SUSY}} = 500 \text{ GeV}$	$\mu = 400 \text{ GeV}$	$M_2 = 240 \text{ GeV}$	$m_0 = 70 \text{ GeV}$

Table 3: SUSY masses, widths, branching ratios, and decay factors η for the benchmark scenario $\text{CP}\chi$, evaluated with `FeynHiggs 2.5.1` [16, 17].

$M_{H_1} = 126.0 \text{ GeV}$	$m_{\tilde{\chi}_1^0} = 118 \text{ GeV}$	$m_{\tilde{e}_R} = 141 \text{ GeV}$	$\text{BR}(\tilde{\chi}_1^+ \rightarrow \ell^+ \tilde{\nu}_\ell) = 11\%$
$M_{H_2} = 492.7 \text{ GeV}$	$m_{\tilde{\chi}_2^0} = 223 \text{ GeV}$	$m_{\tilde{e}_L} = 230 \text{ GeV}$	$\text{BR}(\tilde{\chi}_1^+ \rightarrow W^+ \tilde{\chi}_1^0) = 20\%$
$M_{H_3} = 493.5 \text{ GeV}$	$m_{\tilde{\chi}_3^0} = 405 \text{ GeV}$	$m_{\tilde{\tau}_1} = 138 \text{ GeV}$	$\text{BR}(\tilde{\chi}_1^+ \rightarrow \tilde{\tau}_1 \nu_\tau) = 48\%$
$\Gamma_{H_2} = 1.43 \text{ GeV}$	$m_{\tilde{\chi}_1^\pm} = 223 \text{ GeV}$	$m_{\tilde{\tau}_2} = 232 \text{ GeV}$	$\eta_{\tau^+} = 0.99$
$\Gamma_{H_3} = 1.30 \text{ GeV}$	$m_{\tilde{\chi}_2^\pm} = 425 \text{ GeV}$	$m_{\tilde{\nu}} = 215 \text{ GeV}$	$\eta_{W^+} = -0.30$

and neglect three-body decays. We parametrize the slepton masses by m_0 and M_2 , which enter in the approximate solutions to the renormalization group equations, see Appendix D. For the numerical discussion, we fix $m_0 = 70 \text{ GeV}$. Thus we obtain light sneutrino masses, which enable the chargino decays $\tilde{\chi}_1^\pm \rightarrow \ell^\pm \tilde{\nu}_\ell$. We parametrize the diagonal entries of the squark mass matrices by the common SUSY scale parameter $M_{\text{SUSY}} = M_{\tilde{Q}_3} = M_{\tilde{U}_3} = M_{\tilde{D}_3}$. We fix $M_{\text{SUSY}} = 500 \text{ GeV}$ to suppress Higgs decays into the heavier squarks. In order to reduce the number of parameters, we assume the GUT relation for the gaugino mass parameters $M_1 = 5/3 M_2 \tan^2 \theta_W$. Finally, we choose longitudinal muon beam polarizations of $\mathcal{P}_+ = \mathcal{P}_- = \mathcal{P} = \pm 0.3$, as well as a luminosity of $\mathcal{L} = 1 \text{ fb}^{-1}$. These values should be feasible at a muon collider running at $\sqrt{s} \sim 0.5 \text{ TeV}$ [44].

We center our numerical discussion around scenario $\text{CP}\chi$, defined in Table 2. Inspired by the benchmark scenario CPX [19] for studying enhanced CP-violating Higgs-mixing phenomena, we set $|A| = 2M_{\text{SUSY}} = 1 \text{ TeV}$, $M_3 = 800 \text{ GeV}$, and a non-vanishing phase $\phi_A = 0.2\pi$. We thus obtain large contributions from the trilinear coupling parameter A of the third generation to the Higgs sector, both CP-conserving and CP-violating.

4.1 Conditions for resonant enhanced Higgs mixing

The CP-violating effects are maximized if the mixing of the Higgs states with different CP parities is resonantly enhanced. This can happen naturally in the Higgs decoupling limit. Resonant Higgs mixing occurs when the diagonal elements $m_H^2 - \hat{\Sigma}_{HH}(s)$ and $m_A^2 - \hat{\Sigma}_{AA}(s)$ of the Higgs mass matrix \mathbf{M} , Eq. (4), are similar

in size, and thus their difference is of the same order as the off-diagonal element $\hat{\Sigma}_{HA}(s)$. When $m_H^2 - m_A^2 - \text{Re}[\hat{\Sigma}_{HH}(s) - \hat{\Sigma}_{AA}(s)]$ changes sign, we interpret this condition as a level crossing of the CP eigenstates H and A [13]. The difference of the imaginary parts can be small, $\text{Im}\hat{\Sigma}_{HH}(s) - \text{Im}\hat{\Sigma}_{AA}(s) \approx 0$, if the Higgs channels into heavy squarks are closed, as in our scenario $\text{CP}\chi$. Thus we obtain a large H – A mixing even for moderate values of the CP-violating scalar-pseudoscalar self-energy transitions $\hat{\Sigma}_{HA}(s)$. This also means that, in contrast to the benchmark scenario CPX [19], the Higgs mixing can be large even for small values of μ . We thus choose $\mu = 400$ GeV and $M_2 = 240$ GeV of similar size in order to enhance the branching ratios of the Higgs bosons into lighter charginos, which are large only for mixed gaugino-higgsino charginos. We give the masses of the Higgs bosons, charginos, sneutrinos, light neutralinos, and the widths of the Higgs bosons for scenario $\text{CP}\chi$ in Table 3, where we also list the branching ratios for chargino $\tilde{\chi}_1^+$, and the decay factors η_{τ^+} (D.63) and η_{W^+} (D.62). For non-diagonal chargino production we consider smaller values of μ and M_2 than in scenario $\text{CP}\chi$, in order for this process to be kinematically allowed, while keeping the same remaining parameters.

4.2 Production of $\tilde{\chi}_1^+ \tilde{\chi}_1^-$

4.2.1 \sqrt{s} dependence

For the scenario $\text{CP}\chi$, we analyze the dependence of the asymmetries and the cross sections on the center-of-mass energy \sqrt{s} . The CP-even and CP-odd observables exhibit a characteristic \sqrt{s} dependence, mainly given by the product of Higgs boson propagators $\Delta_{(kl)}$, see Eq. (B.21). A muon collider will have a precise beam energy resolution, and thus enables detailed line-shape scans.

In Fig. 4(a), we show the CP-odd production asymmetry $\mathcal{A}_{11}^{\text{C+P-}}$ (30) for chargino production $\mu^+ \mu^- \rightarrow \tilde{\chi}_1^+ \tilde{\chi}_1^-$ as a function of \sqrt{s} around the heavy Higgs resonances H_2 and H_3 . At the peak value, $\sqrt{s} = (M_{H_2} + M_{H_3})/2 \approx 493$ GeV, the interference of the two nearly degenerate Higgs bosons is maximal, leading to an asymmetry of up to $\mathcal{A}_{11}^{\text{C+P-}} = 30\%$. The asymmetry measures the difference of the chargino production cross section $\sigma_{11}(\mathcal{P})$ for equal positive and negative muon beam polarizations $\mathcal{P} = \pm 0.3$, see Eq. (30). In Fig. 4(b), we show the beam polarization averaged cross section $\sigma_{11}^{\text{C+P+}}$, see Eq. (28), for $\phi_A = 0.2\pi$ (solid), $\phi_A = 0$ (dotted), and $\phi_A = 0.6\pi$ (dash-dotted). We can observe that the splitting of the two resonances is increased in the presence of CP-violating phases in this scenario. For $\phi_A = 0.2\pi$ and $\phi_A = 0.6\pi$ the two resonances are clearly visible in the line shape of the polarization averaged cross section $\sigma_{11}^{\text{C+P+}}$, whereas it assumes the form of a single resonance for $\phi_A = 0$, where the Higgs bosons are extremely degenerate, see Fig. 4(b).

The Higgs boson interference in chargino production also leads to CP-odd and CP-even contributions to the average longitudinal chargino polarizations. In order to analyze the $\tilde{\chi}_1^\pm$ polarization, one can measure the CP-odd asymmetry $\mathcal{A}_{11,\lambda}^{\text{C+P-}}$ (40), and the CP-even asymmetry $\mathcal{A}_{11,\lambda}^{\text{C+P+}}$ (38), of the energy distributions of the decay particle $\lambda = \ell, W$ in the chargino decay $\tilde{\chi}_1^\pm \rightarrow \ell^\pm \tilde{\nu}_\ell^{(*)}$ or $\tilde{\chi}_1^\pm \rightarrow W^\pm \tilde{\chi}_1^0$, respectively.

For simplicity, we discuss only the decay into an electron sneutrino, $\tilde{\chi}_1^\pm \rightarrow e^\pm \tilde{\nu}_e^{(*)}$, i.e. $\lambda = e$. With our choice of slepton sector parameters, i.e., approximate RGE relations for the masses, see Eqs. (D.64)-(D.66), and a vanishing trilinear coupling for the first two slepton generations, the same asymmetries are obtained for the decay into a muon sneutrino, $\lambda = \mu$. The asymmetries for the decay into a tau sneutrino, $\lambda = \tau$, or into a W boson, $\lambda = W$, are obtained by taking into account the decay factors η_τ (D.63) and η_W (D.62), respectively, see Eqs. (39) and (41).

For the decay $\tilde{\chi}_1^\pm \rightarrow e^\pm \tilde{\nu}_e^{(*)}$, we show the \sqrt{s} dependence of the CP- and CPT-odd asymmetry $\mathcal{A}_{11,e}^{C+P-}$ in Fig. 4(c) for $\phi_A = 0.2\pi$. The CP- and CPT-even asymmetry $\mathcal{A}_{11,e}^{C+P+}$ is shown in Fig. 4(d), both for $\phi_A = 0$ and $\phi_A = 0.2\pi$. The phase ϕ_A tends to increase the mass splitting of the Higgs resonances. Their overlap is now reduced, leading in general to a suppression of the CP-even asymmetry $\mathcal{A}_{11,e}^{C+P+}$, in particular at the mean energy of the resonances $\sqrt{s} = (M_{H_2} + M_{H_3})/2$, see the solid line in Fig. 4(d). On the contrary, the larger Higgs splitting increases the CP-odd asymmetries $\mathcal{A}_{11,e}^{C+P-}$ and \mathcal{A}_{11}^{C+P-} .

All asymmetries for production and decay vanish asymptotically far from the resonance region. The continuum contributions from smuon, photon and Z exchange to the difference of the cross sections and to the average chargino polarization cancel in the numerator, but contribute in the denominator of the corresponding asymmetries, see their definitions in Section 3.

In the following Sections, we analyze the dependence of the production cross section and the asymmetries on $|A|$ and ϕ_A , and finally on M_2 and μ , fixing all remaining parameters to those of scenario CP χ . We fix the center-of-mass energy to $\sqrt{s} = (M_{H_2} + M_{H_3})/2$, where we expect the largest CP-odd asymmetries \mathcal{A}_{11}^{C+P-} and $\mathcal{A}_{11,e}^{C+P-}$, see Figs. 4(a) and (c), respectively. For consistency, we also choose $\sqrt{s} = (M_{H_2} + M_{H_3})/2$ for the discussion of the CP-even decay asymmetry $\mathcal{A}_{11,e}^{C+P+}$ although it is generally suppressed at this value if CP is violated.

4.2.2 $|A|$ and ϕ_A dependence

We analyze the dependence of the CP asymmetries on the phase ϕ_A of the trilinear coupling A , which is the only source of CP violation in our study. The CP-odd asymmetries, \mathcal{A}_{11}^{C+P-} and $\mathcal{A}_{11,e}^{C+P-}$ see Fig. 5(a), are approximately maximal, if the mixing of the Higgs states is resonantly enhanced, as discussed in Section 4.1. The degeneracy in the neutral Higgs bosons, however, is lifted by the $H-A$ mixing, as can be observed from Fig. 5(c). A splitting of the order of the Higgs widths $\Gamma_{H_{2,3}}$, shown in Fig. 5(d), leads to large absorptive phases, which are necessary for the presence of CPT-odd observables. The increased Higgs mass splitting leads, however, also to lower peak cross sections, and thus to a lower polarization averaged cross section σ_{11}^{C+P+} , which we show in Fig. 5(b) for common muon beam polarizations $|\mathcal{P}| = 0.3$.

The asymmetries and cross sections for negative ϕ_A can be obtained from symmetry considerations. Since the complex trilinear coupling A is the only source of CP violation in our analysis, the CP-odd asymmetries \mathcal{A}_{11}^{C+P-} and $\mathcal{A}_{11,e}^{C+P-}$ are

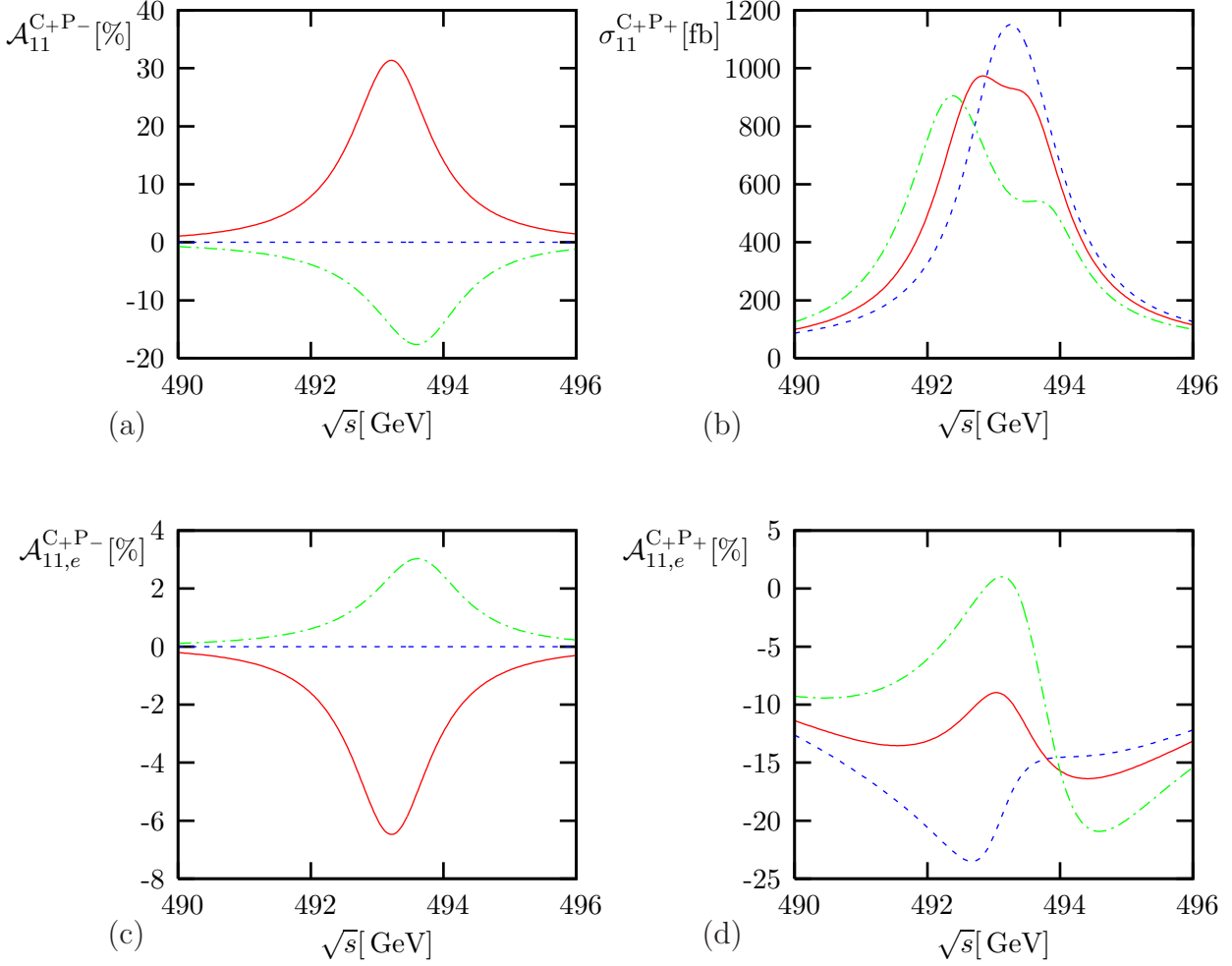


Figure 4: \sqrt{s} dependence of **(a)** the CP-odd production asymmetry \mathcal{A}_{11}^{C+P-} , Eq. (30), and **(b)** the beam polarization averaged cross section σ_{11}^{C+P+} , Eq. (28), for chargino production $\mu^+\mu^- \rightarrow \tilde{\chi}_1^+\tilde{\chi}_1^-$, with common longitudinal beam polarization $|\mathcal{P}| = 0.3$. For the subsequent decay $\tilde{\chi}_1^\pm \rightarrow e^\pm \tilde{\nu}_e^{(*)}$ in **(c)** the CP-odd decay asymmetry $\mathcal{A}_{11,e}^{C+P-}$, Eq. (40), and in **(d)** the CP-even decay asymmetry $\mathcal{A}_{11,e}^{C+P+}$, Eq. (38). The phase of the trilinear coupling A is $\phi_A = 0$ (dotted, blue), $\phi_A = 0.2\pi$ (solid, red), and $\phi_A = 0.6\pi$ (dash-dotted, green). The other SUSY parameters are given in Table 2.

odd with respect to the transformation $\phi_A \rightarrow -\phi_A$, while the CP-even asymmetry $\mathcal{A}_{11,e}^{C+P+}$, and the averaged cross section σ_{11}^{C+P+} , are even.

In Fig. 6, we show contour lines of the averaged cross section σ_{11}^{C+P+} and the asymmetries in the ϕ_A - $|A|$ plane. The largest CP-odd asymmetries \mathcal{A}_{11}^{C+P-} and $\mathcal{A}_{11,e}^{C+P-}$ are obtained for $|A| \approx 2M_{\text{SUSY}} = 1$ TeV. For larger values of $|A|$, the lighter stops become kinematically accessible and H_2 decays dominantly into $\tilde{t}_1^+\tilde{t}_1^-$ pairs. This leads to a suppression of the chargino production cross section, and also to a suppression of the Higgs mixing for small μ . We therefore restrict our discussion to $|A| \lesssim 1$ TeV.

As we have observed in Fig. 5(a), the CP-even asymmetry $\mathcal{A}_{11,e}^{C+P+}$ is in general

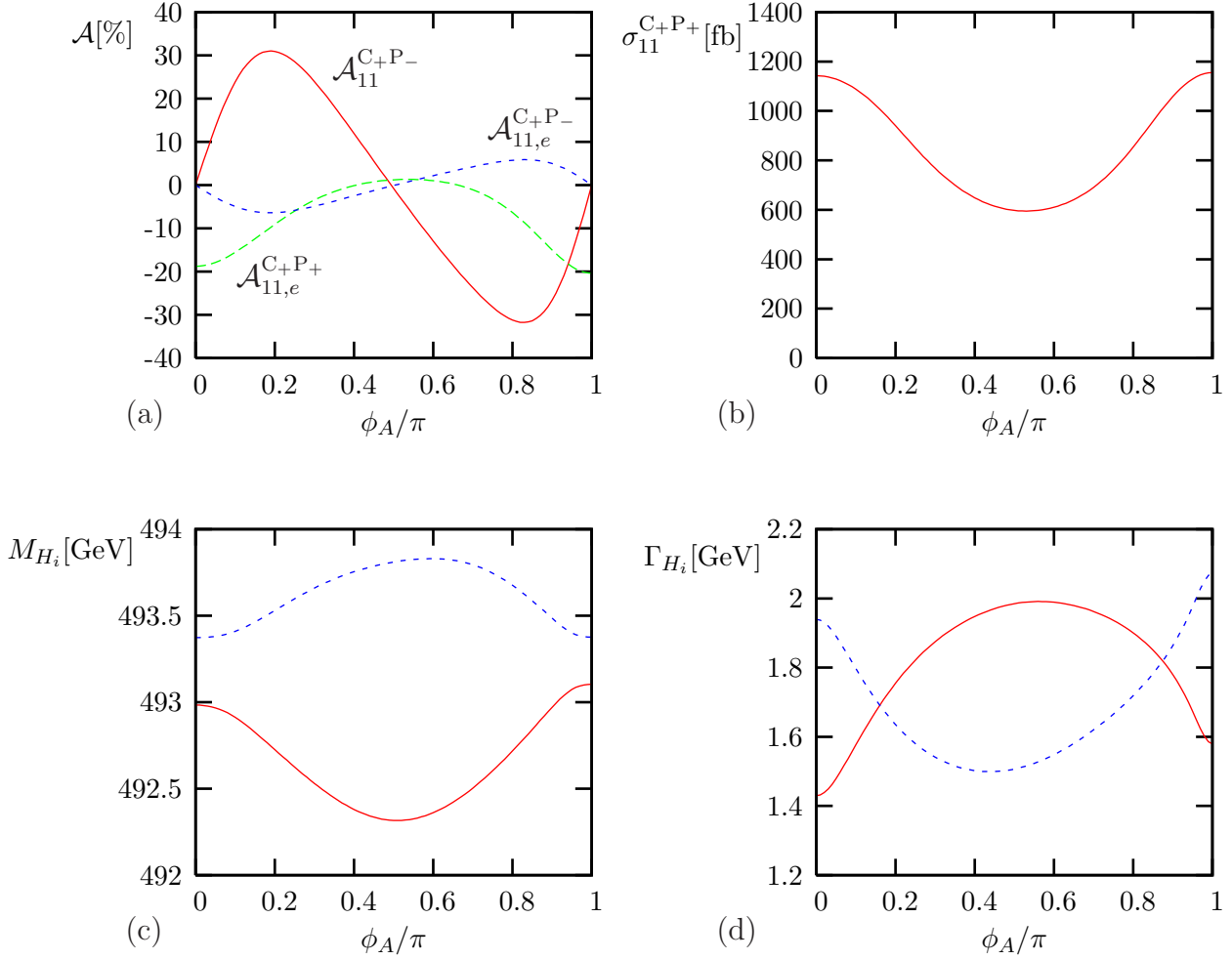


Figure 5: Phase dependence of **(a)** the CP-odd asymmetry \mathcal{A}_{11}^{C+P-} (solid, red), Eq. (30), for chargino production $\mu^+\mu^- \rightarrow \tilde{\chi}_1^+\tilde{\chi}_1^-$ at $\sqrt{s} = (M_{H_2} + M_{H_3})/2$, and for the subsequent decay $\tilde{\chi}_1^\pm \rightarrow e^\pm \tilde{\nu}_e^{(*)}$ the CP-even asymmetry $\mathcal{A}_{11,e}^{C+P+}$ (dashed, green), Eq. (38), and the CP-odd asymmetry $\mathcal{A}_{11,e}^{C+P-}$ (dotted, blue), Eq. (40). In **(b)** the beam polarization averaged cross section σ_{11}^{C+P+} , Eq. (28), with common longitudinal beam polarization $|\mathcal{P}| = 0.3$. In **(c)** the Higgs masses M_{H_i} and **(d)** the Higgs widths Γ_{H_i} , for $i = 2$ (solid, red), and $i = 3$ (dotted, blue). The other SUSY parameters are given in Table 2.

larger in the CP-conserving limit. This can be also seen in Fig. 6(c), where the maximum of the asymmetry is obtained for $\phi_A = 0, \pi$, and $|A| \approx 800$ GeV. However, this is rather coincidental, and is due to the exact degeneracy of the Higgs bosons H and A .

4.2.3 μ and M_2 dependence

The couplings of the Higgs bosons to the charginos strongly depend on the gaugino-higgsino composition of the charginos, which is mainly determined by the values of μ and M_2 . For chargino production $\mu^+\mu^- \rightarrow \tilde{\chi}_1^+\tilde{\chi}_1^-$, we show the CP-odd asymmetry \mathcal{A}_{11}^{C+P-} (30) in the μ - M_2 plane in Fig. 7(a) with $|\mathcal{P}| = 0.3$. The absolute maximal

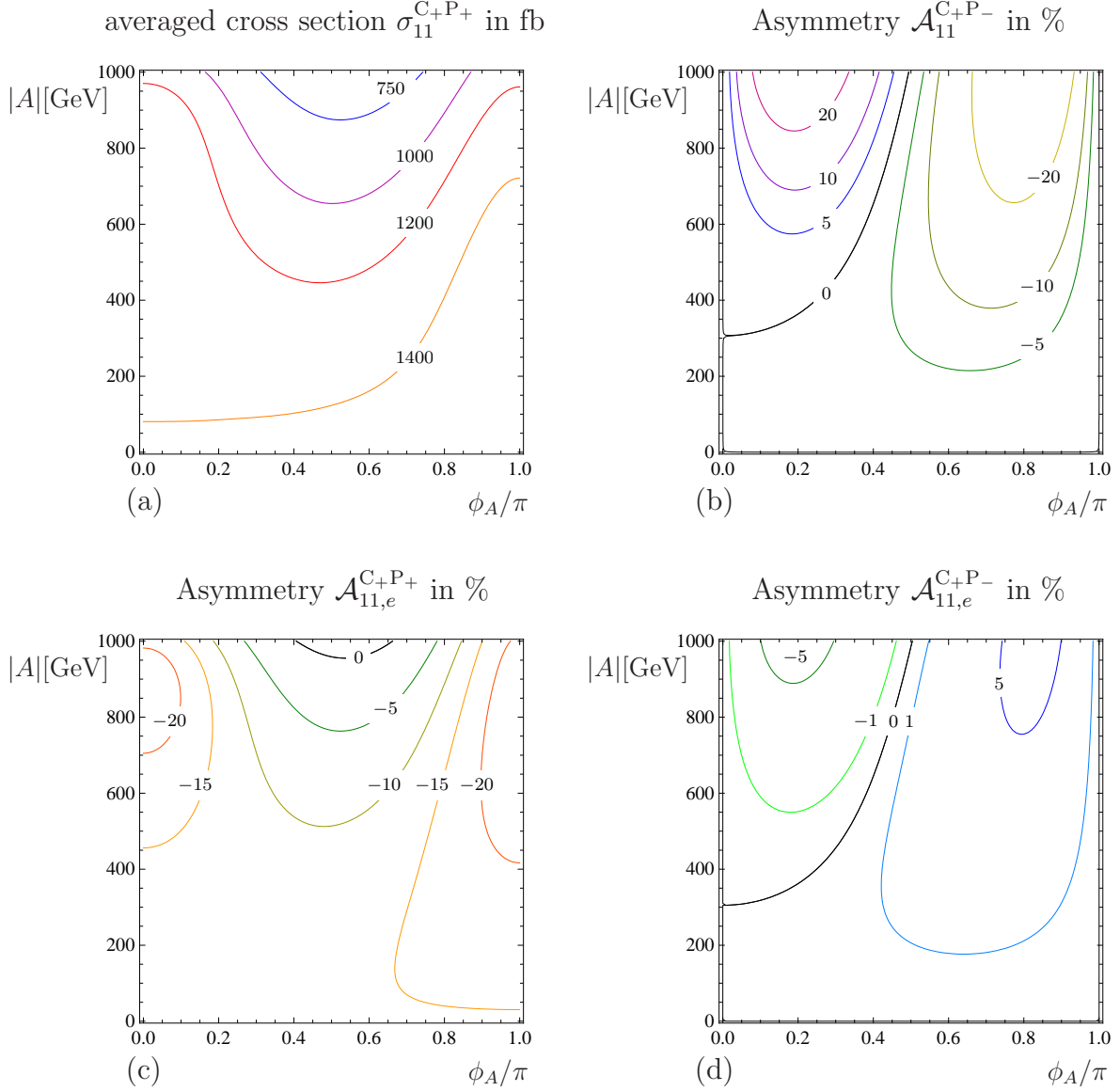


Figure 6: Contour lines in the ϕ_A - $|A|$ plane for chargino production $\mu^+\mu^- \rightarrow \tilde{\chi}_1^+ \tilde{\chi}_1^-$, for (a) the beam polarization averaged cross section σ_{11}^{C+P+} , Eq. (28), and (b) the CP-odd asymmetry \mathcal{A}_{11}^{C+P-} , Eq. (30), at $\sqrt{s} = (M_{H_2} + M_{H_3})/2$ and common longitudinal beam polarization $|\mathcal{P}| = 0.3$. For the subsequent decay $\tilde{\chi}_1^\pm \rightarrow e^\pm \tilde{\nu}_e^{(*)}$, in (c) the CP-even asymmetry $\mathcal{A}_{11,e}^{C+P+}$, Eq. (38), and in (d) the CP-odd asymmetry $\mathcal{A}_{11,e}^{C+P-}$, Eq. (40). The SUSY parameters are given in Table 2.

value of the asymmetry is constrained by the degree of beam polarization. For $|\mathcal{P}| = 0.3$ the maximum would be $\mathcal{A}_{11(\text{max})}^{C+P-} \approx 55\%$, as follows from Eq. (35). We observe in Fig. 7(a) that the asymmetry reaches more than 40% near the chargino production threshold, where the coefficient a_1 (B.16) receives large spin-flip contributions. For smaller μ and M_2 , the Higgs boson widths are increased, since decay channels into light neutralinos and charginos open. This results in a larger overlap of the Higgs resonances, which reduces the absorptive phases, and consequently suppresses the

CP \tilde{T} -odd asymmetry \mathcal{A}_{11}^{C+P-} .

In Fig. 7(c), we show the beam polarization averaged cross section σ_{11}^{C+P+} (28) for chargino production $\mu^+\mu^- \rightarrow \tilde{\chi}_1^+\tilde{\chi}_1^-$, which reaches up to $\sigma_{11}^{C+P+} \approx 2$ pb. In addition the cross section shows no p -wave suppression at threshold, since H_2 and H_3 are mixed CP eigenstates. The corresponding statistical significance, see Eq. (F.71), shown in Fig. 7(b) for an integrated luminosity of $\mathcal{L} = 1 \text{ fb}^{-1}$, is largest near threshold. In Fig. 7(d), we show the branching ratio for the chargino decay $\tilde{\chi}_1^+ \rightarrow e^+\tilde{\nu}_e$, which reaches more than 15%, as the leptonic decay modes into μ and τ . The main competing channels are the decay into the W boson, and those into sleptons \tilde{e}_L , $\tilde{\mu}_L$, and $\tilde{\tau}_{1,2}$, see Eq. (44). The chargino decay $\tilde{\chi}_1^+ \rightarrow \tilde{\tau}_1^+\nu_\tau$ is dominating, see the branching ratios in Table 3, and is the only two-body decay channel for $m_{\tilde{\chi}_1^\pm} < m_{\tilde{\nu}_\ell}$, see the contour of the kinematical threshold in Fig. 7(d).

For the chargino decay $\tilde{\chi}_1^\pm \rightarrow e^\pm\tilde{\nu}_e$, we show the CP-odd and CP-even decay asymmetries $\mathcal{A}_{11,e}^{C+P-}$ (40), and $\mathcal{A}_{11,e}^{C+P+}$ (38), in Figs. 8(a) and (b), respectively. As discussed before, the CP-even asymmetry $\mathcal{A}_{11,e}^{C+P+}$ is suppressed by CP-violating effects due to the smaller overlap of the resonances at $\sqrt{s} = (M_{H_2} + M_{H_3})/2$. Therefore we only find large values of $\mathcal{A}_{11,e}^{C+P+}$ for light neutralinos and charginos in the lower left corner of Fig. 8(b), where the larger Higgs widths counter the effect of the larger Higgs mass difference. On the contrary, in that region the CP-odd asymmetry $\mathcal{A}_{11,e}^{C+P-}$ is reduced due to smaller absorptive phases. Finally, at threshold the longitudinal polarization of the chargino Σ_{res}^3 (18) vanishes, and thus also both decay asymmetries, as follows from Eqs. (B.17) and (B.18).

The statistical significances of the CP-odd and CP-even decay asymmetries $\mathcal{A}_{11,e}^{C+P-}$, and $\mathcal{A}_{11,e}^{C+P+}$, see Eqs. (F.73), (F.74), reach at most $\mathcal{S}_{11}^{C+P-} \approx 2$ and $\mathcal{S}_{11}^{C+P+} \approx 3$ respectively, for an integrated luminosity of $\mathcal{L} = 1 \text{ fb}^{-1}$. Thus their measurement will be challenging. Nonetheless, only these asymmetries allow to disentangle the contributions b_0^+ and b_1^+ to the longitudinal chargino polarization Σ_{res}^3 (18). However these asymmetries can also be measured in the decays $\tilde{\chi}_1^\pm \rightarrow W^\pm\tilde{\chi}_1^0$, and $\tilde{\chi}_1^\pm \rightarrow \tau^\pm\tilde{\nu}_\tau^{(*)}$. Note that the corresponding decay asymmetries are smaller due to the decay factors η_λ , which are of the order $|\eta_{W^\pm}| \approx 0.2 - 0.4$ and $|\eta_{\tau^\pm}| \approx 1$. A measurement of the asymmetries in these decay channels is more involved, since the W and τ reconstruction efficiencies have to be taken into account.

4.2.4 Comparison with asymmetries in neutralino production

The results obtained for diagonal chargino production $\mu^+\mu^- \rightarrow \tilde{\chi}_1^+\tilde{\chi}_1^-$ in the previous section have similarities with the corresponding asymmetries for neutralino production, see Ref. [7], and Ref. [42] for a detailed review. For instance, we have obtained similar line-shapes of the CP-odd production asymmetry, \mathcal{A}_{11}^{C+P-} , Eq. (30), as well as of the CP-odd and CP-even asymmetries for the chargino decays $\mathcal{A}_{11,e}^{C+P-}$, Eq. (40), and $\mathcal{A}_{11,e}^{C+P+}$, Eq. (38), respectively, compared with the analogous asymmetries for neutralino production. The asymmetries also show a very similar dependence on the common complex trilinear coupling parameter A , as well as on the parameters

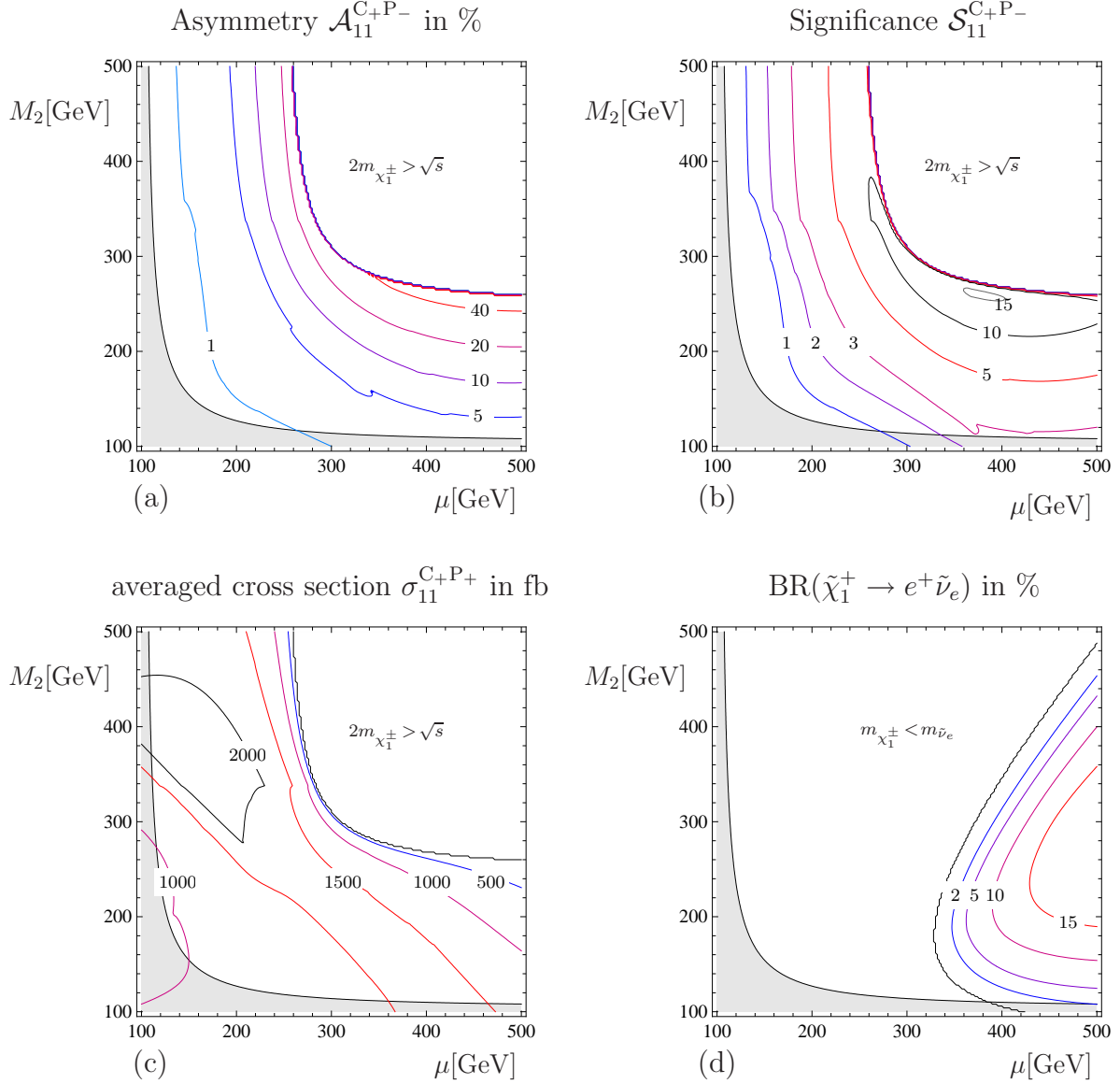


Figure 7: **(a)-(c)** Chargino production $\mu^+\mu^- \rightarrow \tilde{\chi}_1^+\tilde{\chi}_1^-$ at $\sqrt{s} = (M_{H_2} + M_{H_3})/2$ with common muon beam polarization $|\mathcal{P}| = 0.3$. Contour lines in the μ - M_2 plane for **(a)** the CP-odd asymmetry \mathcal{A}_{11}^{C+P-} , Eq. (30), **(b)** the corresponding significance \mathcal{S}_{11}^{C+P-} , Eq. (F.71), with $\mathcal{L} = 1 \text{ fb}^{-1}$, and **(c)** the beam polarization averaged cross section σ_{11}^{C+P+} , Eq. (28), for the SUSY parameters as given in Table 2. The chargino branching ratio $\text{BR}(\tilde{\chi}_1^+ \rightarrow e^+ \tilde{\nu}_e)$ is given in **(d)**. The shaded area is excluded by $m_{\tilde{\chi}_1^\pm} < 103$ GeV.

μ and M_2 . In both processes, the production asymmetry is enhanced at threshold, whereas the decay asymmetries show a distinct p -wave suppression. The similarities are due to similar kinematics, i.e., production of spin-half charginos or neutralinos, as well as dynamics, i.e., Higgs interference in the production of a C-even final state of massive gauginos and higgsinos.

Note that for neutralino or diagonal chargino production only C-even production asymmetries can be defined, whereas after including the C-odd decay, only C-odd

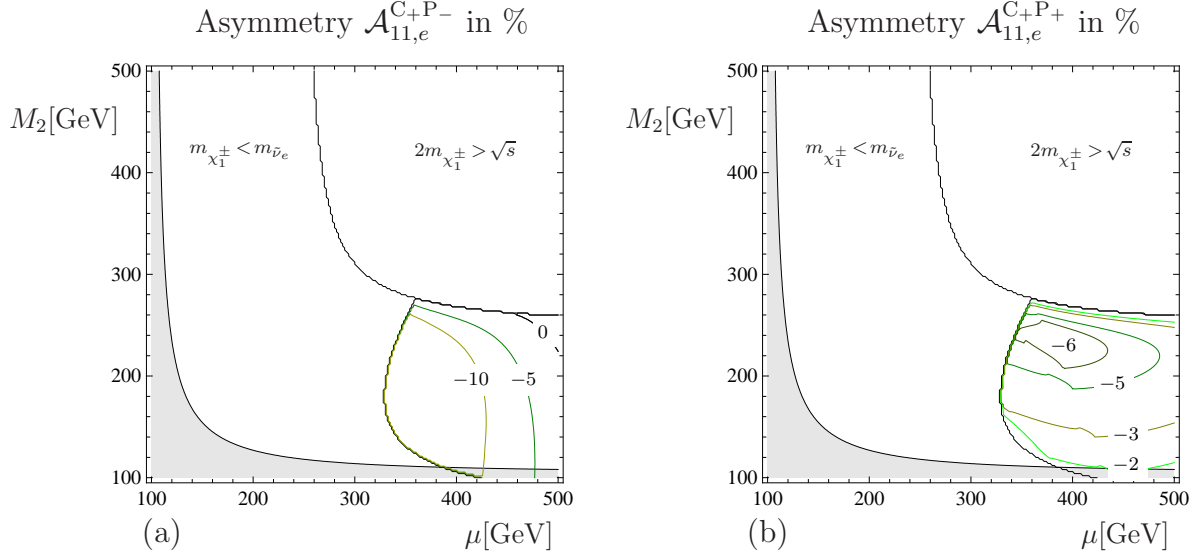


Figure 8: Contour lines in the μ - M_2 plane for **(a)** the CP-odd asymmetry $\mathcal{A}_{11,e}^{C+P-}$, Eq. (40), and **(b)** the CP-even asymmetry $\mathcal{A}_{11,e}^{C+P+}$, Eq. (38), for chargino production $\mu^+\mu^- \rightarrow \tilde{\chi}_1^+\tilde{\chi}_1^-$ and decay $\tilde{\chi}_1^\pm \rightarrow e^\pm\tilde{\nu}_e^{(*)}$ at $\sqrt{s} = (M_{H_2} + M_{H_3})/2$ with longitudinally muon beam polarization $|\mathcal{P}| = 0.3$, for the SUSY parameters as given in Table 2. The corresponding chargino cross section and branching ratio are shown in Fig. 7. The shaded area is excluded by $m_{\chi_1^\pm} < 103$ GeV.

decay asymmetries can be probed, see also the detailed discussions in Section 3. For non-diagonal chargino production, in addition two C-odd production asymmetries, as well as two C-even decay asymmetries, are accessible, which we discuss in the following section.

4.3 Production of $\tilde{\chi}_1^\pm\tilde{\chi}_2^\mp$

For non-diagonal chargino production, $\mu^+\mu^- \rightarrow \tilde{\chi}_1^\pm\tilde{\chi}_2^\mp$, we study the μ - M_2 dependence of the cross section, and of the CP-odd and CP-even production asymmetries \mathcal{A}_{12}^{C+P-} , Eq. (30), and \mathcal{A}_{12}^{C-P-} , Eq. (32), respectively. The CP-odd asymmetry \mathcal{A}_{12}^{C+P-} is largest at threshold, where it reaches up to -10% , see Fig. 9(a). Since the beam polarization averaged cross section reaches up to 400 fb in that region, we obtain a significance of $\mathcal{S}_{12}^{C+P-} < 3$, for an integrated luminosity of $\mathcal{L} = 1 \text{ fb}^{-1}$, see Fig. 9(c). The CP-even production asymmetry exhibits a characteristic $\mu \leftrightarrow M_2$ symmetry, see Fig. 9(d). The Higgs chargino couplings transform as $c_{L,R}^{H_k\chi_1\chi_2} \leftrightarrow c_{L,R}^{H_k\chi_2\chi_1}$ (13) under $\mu \leftrightarrow M_2$, resulting in a sign change of \mathcal{A}_{12}^{C-P-} [33]. Consequently, for $\mu = M_2$ the asymmetry vanishes, see the zero contour in Fig. 9(d). On the other hand, the asymmetry is nearly maximal for $\mu \gg M_2$ or $\mu \ll M_2$, see the upper left and lower right corners of Fig. 9(d). The maximum absolute value would be $\mathcal{A}_{12(\text{max})}^{C-P-} \approx 55\%$, see Eq. (35) with $|\mathcal{P}| = 0.3$. We do not show the CP-odd production asymmetry \mathcal{A}_{12}^{C-P+} , Eq. (31), which is only of order 1% near threshold.

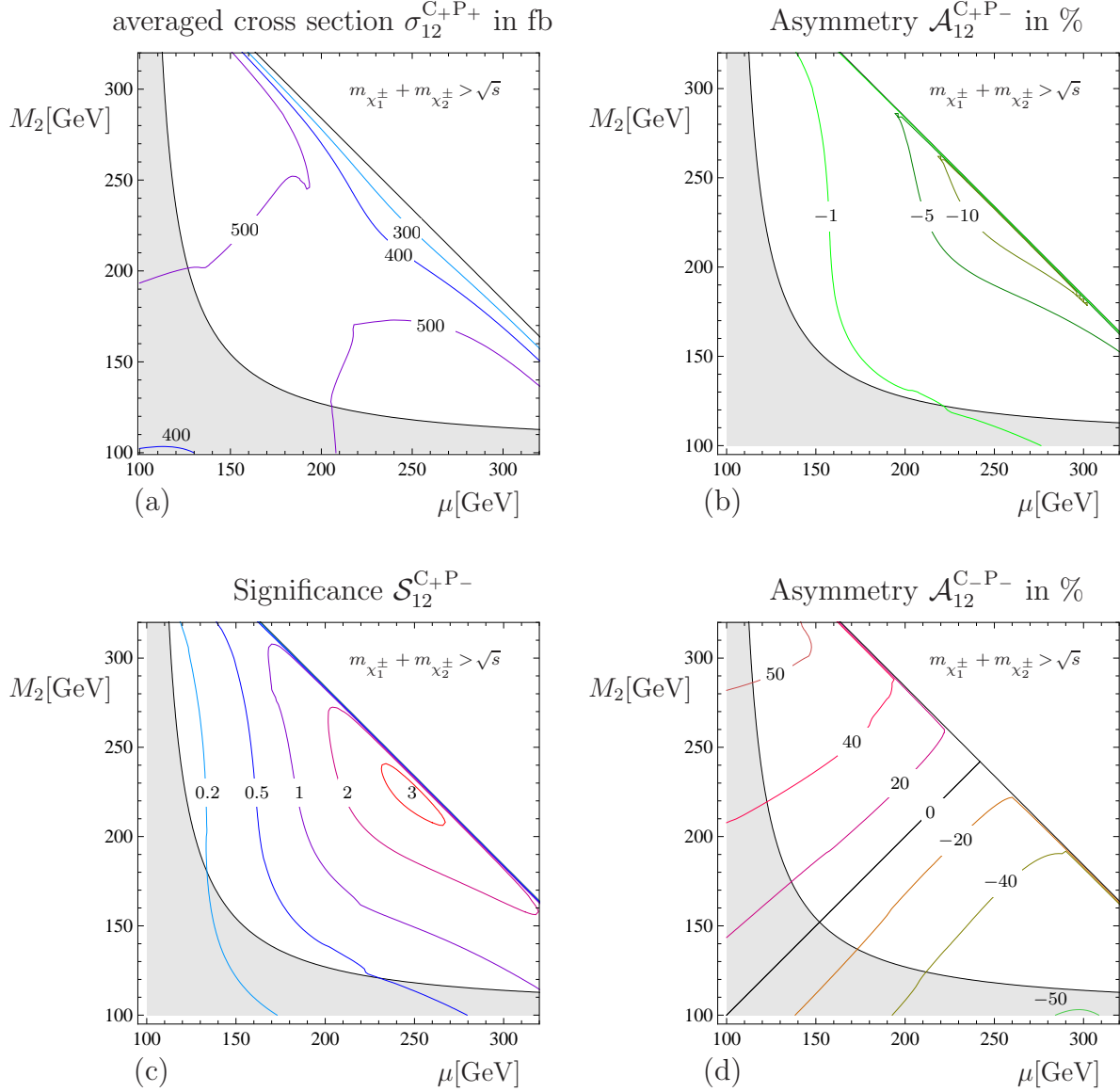


Figure 9: Chargino production $\mu^+\mu^- \rightarrow \tilde{\chi}_1^\pm \tilde{\chi}_2^\mp$ at $\sqrt{s} = (M_{H_2} + M_{H_3})/2$ with common muon beam polarization $|\mathcal{P}| = 0.3$. Contour lines in the μ - M_2 plane for **(a)** the beam polarization averaged cross section σ_{12}^{C+P+} , Eq. (28), **(b)** the CP-odd asymmetry \mathcal{A}_{12}^{C+P-} , Eq. (30), **(c)** the corresponding significance \mathcal{S}_{12}^{C+P-} , Eq. (F.71), with $\mathcal{L} = 1 \text{ fb}^{-1}$, and **(d)** the CP-even asymmetry \mathcal{A}_{12}^{C-P-} , Eq. (32). The SUSY parameters are given in Table 2. The shaded area is excluded by $m_{\tilde{\chi}_1^\pm} < 103 \text{ GeV}$.

For the subsequent chargino decay $\tilde{\chi}_2^\pm \rightarrow e^\pm \tilde{\nu}_e^{(*)}$, we show the CP-even decay asymmetries $\mathcal{A}_{12,e}^{C+P+}$, Eq. (38), and $\mathcal{A}_{12,e}^{C-P-}$, Eq. (42), in Fig. 10. Both asymmetries are large in a wide region of the μ - M_2 parameter space. The asymmetry $\mathcal{A}_{12,e}^{C-P-}$ also exhibits the characteristic $\mu \leftrightarrow M_2$ symmetry, see Fig. 10(b), as discussed above for the production asymmetry \mathcal{A}_{12}^{C-P-} . The decay asymmetry however has also contributions from the continuum polarization $\bar{\Sigma}_{\text{cont}}^3$, see Eq. (43). Thus the zero contour in Fig. 10(b) gets slightly shifted from $\mu = M_2$. Since the continuum contributions

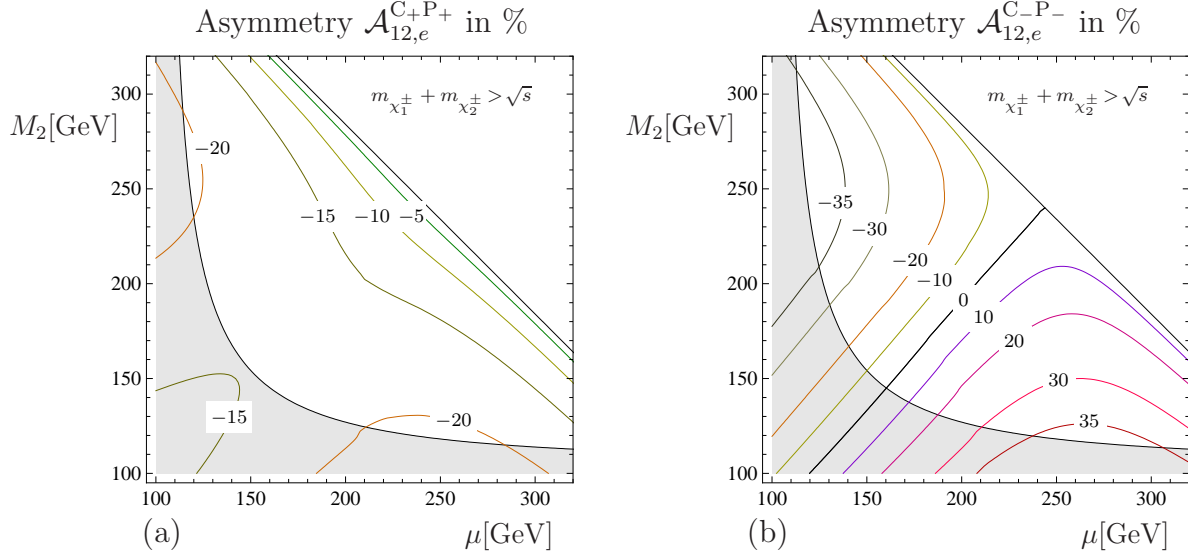


Figure 10: Chargino production $\mu^+\mu^- \rightarrow \tilde{\chi}_1^\pm \tilde{\chi}_2^\mp$ at $\sqrt{s} = (M_{H_2} + M_{H_3})/2$ with common muon beam polarization $|\mathcal{P}| = 0.3$, and subsequent chargino decay $\tilde{\chi}_2^\pm \rightarrow e^\pm \tilde{\nu}_e^{(*)}$. Contour lines in the μ - M_2 plane for the CP-even decay asymmetries **(a)** $\mathcal{A}_{12,e}^{C+P+}$, Eq. (38), and **(b)** $\mathcal{A}_{12,e}^{C-P-}$, Eq. (42), for the SUSY parameters as given in Table 2. The corresponding chargino production cross section is shown in Fig. 9. The shaded area is excluded by $m_{\chi_1^\pm} < 103$ GeV.

are small compared to those from the resonance, the $\mu \leftrightarrow M_2$ symmetry of $\mathcal{A}_{12,e}^{C-P-}$, however, still holds approximately.

The chargino $\tilde{\chi}_2^\pm$ two-body decays are open in the entire μ - M_2 plane, with branching ratios up to $\text{BR}(\tilde{\chi}_2^+ \rightarrow e^+ \tilde{\nu}_e) = 10\%$. Other competing channels are $\tilde{\chi}_2^+ \rightarrow W^+ \tilde{\chi}_1^0$ and $\tilde{\chi}_2^+ \rightarrow \tau^+ \tilde{\nu}_\tau$, with branching ratios of also up to 10%. For these decay channels the asymmetries $\mathcal{A}_{12,W}^{C+P\pm}$ and $\mathcal{A}_{12,\tau}^{C+P\pm}$ are accessible. Here, the appropriate decay factors η_W (D.62) and η_τ (D.63), respectively, have to be taken into account. The CP-odd decay asymmetries $\mathcal{A}_{12,e}^{C+P-}$, Eq. (40), and $\mathcal{A}_{12,e}^{C-P+}$, Eq. (38), do not exceed 0.2%.

5 Summary and conclusions

In the MSSM with CP violation in the Higgs sector, we have studied chargino production at the muon collider around the resonances of the two heavy neutral Higgs bosons. For nearly degenerate neutral Higgs bosons, as in the Higgs decoupling limit, the CP-violating Higgs mixing can be resonantly enhanced, which allows for large CP-violating effects. We have defined the complete set of CP observables to study the Higgs interference and their radiatively induced Higgs mixings. The muon collider with a precisely tunable beam energy is an ideal tool to study the strong \sqrt{s} dependence of the CP asymmetries.

Using longitudinally polarized muon beams, we have classified the set of CP-even and CP-odd asymmetries for chargino production, as well as for the chargino decays into leptons. Appropriate observables can be defined for the decays into W bosons. In contrast to the production asymmetries, the asymmetries of the decay probe the longitudinal chargino polarization. Due to spin correlations between production and decay, the chargino polarization depends sensitively on the Higgs interference. Thus a different and independent set of asymmetries sensitive to the Higgs couplings can be defined, that complement the production asymmetries.

In a numerical study, we have parametrized CP violation in the Higgs sector by a common phase ϕ_A of the trilinear scalar coupling parameter. We have analyzed the dependence of the asymmetries and cross sections on the complex parameter A , as well as on the (real) gaugino parameters μ and M_2 . Large CP-violating asymmetries are obtained if the H - A Higgs mixing is resonantly enhanced. We have discussed the conditions necessary for such a resonant mixing. It occurs naturally in the Higgs decoupling limit, when the Higgs mass difference is of the order of their widths. We have identified the appropriate class of scenarios which are adequate to study chargino production and decays.

For $\tilde{\chi}_1^+ \tilde{\chi}_1^-$ production, the largest CP-odd production asymmetry can go up to 40% for a degree of beam polarization of $\mathcal{P} = 0.3$. The CP-odd decay asymmetry for the subsequent chargino decay reaches up to 10%. By comparing the asymmetries to the results which are known in the literature from non-diagonal neutralino production, we have observed striking similarities. They are due to similar kinematics, i.e., production of spin-half charginos or neutralinos, as well as to the dynamics, i.e., Higgs interference in the production of a C-even final state of fermions. We have completed the numerical study with the discussion of non-diagonal chargino production. Here, the C-odd and CP-even asymmetries are almost maximal and reach more than 50% for a degree of beam polarization of $\mathcal{P} = 0.3$.

We find that chargino and neutralino pair production at a muon collider is complementary to similar studies for the production of Standard Model fermions. While $t\bar{t}$ production is favored for small values of $\tan\beta$, third generation fermion production is largest for large $\tan\beta$. The strong effect of the CP phases on the Higgs mixing, and thus on their masses, leads to a center-of-mass energy dependence of the observables which can be ideally studied at the muon collider.

We conclude that chargino production at the muon collider is the ideal testing ground to analyze and comprehend the phenomenology of MSSM Higgs mixing in the presence of CP-violating phases. In particular, the crucial interference effects of the two nearly degenerated heavy neutral Higgs resonances can well be analyzed and understood. The proposed set of CP-sensitive observables allows for a systematic test of the CP nature of the heavy neutral Higgs resonances, and their couplings to charginos.

6 Acknowledgments

We thank Sven Heinemeyer, Herbi Dreiner and Karina Williams for helpful comments and discussions. OK was supported by the SFB Transregio 33: The Dark Universe. FP thanks the Grid Infrastructure of the EUFORIA project (FP7 Contract 211804). OK thanks the Instituto de Física de Cantabria (IFCA) for kind hospitality, where part of this work was completed.

Appendix

A Density matrix formalism

We use the spin density matrix formalism [42,50,51] for the calculation of the squared amplitudes for chargino production, Eq. (1), and decay channels, Eqs. (2) and (3). The amplitude for chargino production via resonant Higgs exchange, Eq. (15), depends on the helicities λ_{\pm} of the muons μ^{\pm} and the helicities λ_i, λ_j of the produced charginos, $\mu^+ \mu^- \rightarrow \tilde{\chi}_i^- \tilde{\chi}_j^+$,

$$T_{\lambda_i \lambda_j \lambda_+ \lambda_-}^P = \Delta(H_k) \left[\bar{v}(p_{\mu^+}, \lambda_+) \left(c_L^{H_k \mu \mu} P_L + c_R^{H_k \mu \mu} P_R \right) u(p_{\mu^-}, \lambda_-) \right] \\ \times \left[\bar{u}(p_{\tilde{\chi}_j^+}, \lambda_j) \left(c_L^{H_k \chi_i \chi_j} P_L + c_R^{H_k \chi_i \chi_j} P_R \right) v(p_{\tilde{\chi}_i^-}, \lambda_i) \right]. \quad (\text{A.1})$$

We include the longitudinal beam polarizations of the muon-beams, \mathcal{P}_- and \mathcal{P}_+ , with $-1 \leq \mathcal{P}_{\pm} \leq +1$ in their density matrices

$$\rho_{\lambda_- \lambda'_-}^- = \frac{1}{2} \left(\delta_{\lambda_- \lambda'_-} + \mathcal{P}_- \tau_{\lambda_- \lambda'_-}^3 \right), \quad (\text{A.2})$$

$$\rho_{\lambda_+ \lambda'_+}^+ = \frac{1}{2} \left(\delta_{\lambda_+ \lambda'_+} + \mathcal{P}_+ \tau_{\lambda_+ \lambda'_+}^3 \right), \quad (\text{A.3})$$

where τ^3 is the third Pauli matrix. The unnormalized spin density matrix of $\tilde{\chi}_i^- \tilde{\chi}_j^+$ production and $\tilde{\chi}_j^+$ decay are given by,

$$\rho_{\lambda_j \lambda'_j}^P = \sum_{\lambda_i, \lambda_+, \lambda'_+, \lambda_- \lambda'_-} \rho_{\lambda_+ \lambda'_+}^+ \rho_{\lambda_- \lambda'_-}^- T_{\lambda_i \lambda_j \lambda_+ \lambda_-}^P T_{\lambda_i \lambda'_j \lambda'_+ \lambda'_-}^{P*}, \quad (\text{A.4})$$

$$\rho_{\lambda'_j \lambda_j}^D = T_{\lambda'_j}^{D*} T_{\lambda_j}^D. \quad (\text{A.5})$$

The amplitude squared for production and decay is then

$$|T|^2 = |\Delta(\tilde{\chi}_j^+)|^2 \sum_{\lambda_j \lambda'_j} \rho_{\lambda_j \lambda'_j}^P \rho_{\lambda'_j \lambda_j}^D, \quad (\text{A.6})$$

with the chargino propagator

$$\Delta(\tilde{\chi}_j^+) = \frac{i}{p_{\chi_j^+}^2 - m_{\chi_j^+}^2 + i m_{\chi_j^+} \Gamma_{\chi_j^+}}. \quad (\text{A.7})$$

The spin density matrices, Eqs. (A.4) and (A.5), can be expanded in terms of the Pauli matrices τ^a

$$\rho_{\lambda_j \lambda'_j}^P = \delta_{\lambda_j \lambda'_j} P + \sum_{a=1}^3 \tau_{\lambda_j \lambda'_j}^a \Sigma_P^a, \quad (\text{A.8})$$

$$\rho_{\lambda'_j \lambda_j}^D = \delta_{\lambda'_j \lambda_j} D + \sum_{a=1}^3 \tau_{\lambda'_j \lambda_j}^a \Sigma_D^a, \quad (\text{A.9})$$

where we have defined a set of chargino spin vectors $s_{\chi_j^+}^a$. In the center-of-mass system, they are

$$s_{\chi_j^+}^{1,\mu} = (0; 1, 0, 0), \quad s_{\chi_j^+}^{2,\mu} = (0; 0, 1, 0), \quad s_{\chi_j^+}^{3,\mu} = \frac{1}{m_{\chi_j^+}} (|\vec{p}_{\chi_j^+}|; 0, 0, E_{\chi_j^+}). \quad (\text{A.10})$$

We have chosen a coordinate frame such that the momentum of the chargino $\tilde{\chi}_j^+$ is

$$p_{\chi_j^+}^\mu = (E_{\chi_j^+}; 0, 0, |\vec{p}_{\chi_j^+}|), \quad (\text{A.11})$$

with

$$E_{\chi_j^+} = \frac{s + m_{\chi_j^+}^2 - m_{\chi_i^+}^2}{2\sqrt{s}}, \quad |\vec{p}_{\chi_j^+}| = \frac{\sqrt{\lambda_{ij}}}{2\sqrt{s}}, \quad (\text{A.12})$$

and the triangle function

$$\lambda_{ij} = \lambda(s, m_{\chi_i^+}^2, m_{\chi_j^+}^2), \quad (\text{A.13})$$

with $\lambda(x, y, z) = x^2 + y^2 + z^2 - 2(xy + xz + yz)$. Inserting the density matrices, Eqs. (A.8) and (A.9), into Eq. (A.6), gives the amplitude squared in the form of Eq. (15).

B Higgs exchange contributions

We have expressed the resonant contributions to the spin-density matrix coefficients as functions of the longitudinal μ^+ and μ^- beam polarizations, Eqs. (17) and (18),

$$\begin{aligned} P_{\text{res}} &= (1 + \mathcal{P}_+ \mathcal{P}_-) a_0 + (\mathcal{P}_+ + \mathcal{P}_-) a_1, \\ \Sigma_{\text{res}}^3 &= (1 + \mathcal{P}_+ \mathcal{P}_-) b_0 + (\mathcal{P}_+ + \mathcal{P}_-) b_1. \end{aligned}$$

The coefficients a_n and b_n on the r.h.s. are

$$a_n = \sum_{l, k \leq l} (2 - \delta_{kl}) a_n^{kl}, \quad b_n = \sum_{l, k \leq l} (2 - \delta_{kl}) b_n^{kl}, \quad n = 0, 1; \quad (\text{B.14})$$

with the sum over the contributions from the Higgs bosons H_k, H_l with $k, l = 1, 2, 3$, respectively, and [7]

$$a_0^{kl} = \frac{s}{2} |\Delta_{(kl)}| \left[|c_\mu^+| |c_\chi^+| f_{ij} \cos(\delta_\mu^+ + \delta_\chi^+ + \delta_\Delta) \right]$$

$$- |c_\mu^+| |c_\chi^{RL}| m_i m_j \cos(\delta_\mu^+ + \delta_\chi^{RL} + \delta_\Delta) \Big]_{(kl)}, \quad (\text{B.15})$$

$$a_1^{kl} = \frac{s}{2} |\Delta_{(kl)}| \left[|c_\mu^-| |c_\chi^+| f_{ij} \cos(\delta_\mu^- + \delta_\chi^+ + \delta_\Delta) - |c_\mu^-| |c_\chi^{RL}| m_i m_j \cos(\delta_\mu^- + \delta_\chi^{RL} + \delta_\Delta) \right]_{(kl)}, \quad (\text{B.16})$$

$$b_0^{kl} = -\frac{s}{4} |\Delta_{(kl)}| \left[|c_\mu^+| |c_\chi^-| \sqrt{\lambda_{ij}} \cos(\delta_\mu^+ + \delta_\chi^- + \delta_\Delta) \right]_{(kl)}, \quad (\text{B.17})$$

$$b_1^{kl} = -\frac{s}{4} |\Delta_{(kl)}| \left[|c_\mu^-| |c_\chi^-| \sqrt{\lambda_{ij}} \cos(\delta_\mu^- + \delta_\chi^- + \delta_\Delta) \right]_{(kl)}. \quad (\text{B.18})$$

We have defined the products of couplings, suppressing the chargino indices i and j ,

$$c_{\alpha(kl)}^\pm = c_R^{H_k \alpha \alpha} c_R^{H_l \alpha \alpha^*} \pm c_L^{H_k \alpha \alpha} c_L^{H_l \alpha \alpha^*} = \left[|c_\alpha^\pm| \exp(i\delta_\alpha^\pm) \right]_{(kl)}, \quad \alpha = \mu, \chi, \quad (\text{B.19})$$

$$c_{\chi(kl)}^{RL} = c_R^{H_k \chi \chi} c_L^{H_l \chi \chi^*} + c_L^{H_k \chi \chi} c_R^{H_l \chi \chi^*} = \left[|c_\chi^{RL}| \exp(i\delta_\chi^{RL}) \right]_{(kl)}, \quad (\text{B.20})$$

the product of the Higgs boson propagators (8),

$$\Delta_{(kl)} = \Delta(H_k) \Delta(H_l)^* = \left[|\Delta| \exp(i\delta_\Delta) \right]_{(kl)}, \quad (\text{B.21})$$

and the kinematical functions $f_{ij} = (s - m_{\chi_i^-}^2 - m_{\chi_j^+}^2)/2$, and λ_{ij} , see Eq. (A.13). We neglect interferences of the chirality violating Higgs exchange amplitudes with the chirality conserving continuum amplitudes, which are of order m_μ/\sqrt{s} . The contributions from H_1 exchange are small far from its resonance.

Note that the longitudinal chargino polarization, parametrized by the coefficients b_0 and b_1 of Σ_{res}^3 , see Eqs. (B.17) and (B.18), vanishes at threshold as $\sqrt{\lambda_{ij}}$. We have defined b_0 and b_1 for the longitudinal polarization of the positively charged chargino $\tilde{\chi}_j^+$ in the reaction $\mu^+ \mu^- \rightarrow \tilde{\chi}_i^- \tilde{\chi}_j^+$. The coefficients are the same for the other produced chargino $\tilde{\chi}_i^-$, due to angular momentum conservation.

C Continuum contributions

The non-resonant chargino production (1) proceeds via γ and Z boson exchange in the s -channel, and muon-sneutrino $\tilde{\nu}_\mu$ exchange in the t -channel, see the Feynman diagrams in Fig. 2. The MSSM interaction Lagrangians are [1, 51]:

$$\mathcal{L}_{Z^0 \mu \bar{\mu}} = -\frac{g}{\cos \theta_W} Z_\nu^0 \bar{\mu} \gamma^\nu [L_\mu P_L + R_\mu P_R] \mu, \quad (\text{C.22})$$

$$\mathcal{L}_{\gamma \tilde{\chi}^+ \tilde{\chi}^-} = -e A_\nu \tilde{\chi}_i^+ \gamma^\nu \tilde{\chi}_j^- \delta_{ij}, \quad e > 0, \quad (\text{C.23})$$

$$\mathcal{L}_{Z^0 \tilde{\chi}^+ \tilde{\chi}^-} = \frac{g}{\cos \theta_W} Z_\mu \tilde{\chi}_i^+ \gamma^\mu [O_{ij}^{\prime L} P_L + O_{ij}^{\prime R} P_R] \tilde{\chi}_j^-, \quad (\text{C.24})$$

$$\mathcal{L}_{\ell \tilde{\nu} \tilde{\chi}^+} = -g V_{i1}^* \tilde{\chi}_i^+ P_L \ell \tilde{\nu}^* + \text{h.c.}, \quad \ell = e, \mu, \quad (\text{C.25})$$

with $i, j = 1, 2$ and $P_{L,R} = (1 \mp \gamma_5)/2$. The couplings are [1, 51]

$$L_\mu = -\frac{1}{2} + \sin^2 \theta_W, \quad R_\mu = \sin^2 \theta_W, \quad (\text{C.26})$$

$$O'_{ij}{}^L = -V_{i1}V_{j1}^* - \frac{1}{2}V_{i2}V_{j2}^* + \delta_{ij}\sin^2 \theta_W, \quad (\text{C.27})$$

$$O'_{ij}{}^R = -U_{i1}^*U_{j1} - \frac{1}{2}U_{i2}^*U_{j2} + \delta_{ij}\sin^2 \theta_W, \quad (\text{C.28})$$

with the weak mixing angle θ_W , and the weak coupling constant $g = e/\sin \theta_W$, $e > 0$. The complex unitary 2×2 matrices U_{mn} and V_{mn} diagonalize the chargino mass matrix $X_{\alpha\beta}$, $U_{m\alpha}^*X_{\alpha\beta}V_{\beta n}^{-1} = m_{\chi_n^\pm}\delta_{mn}$, with $m_{\chi_n^\pm} > 0$.

The helicity amplitudes for γ , Z and $\tilde{\nu}_\mu$ exchange are

$$\begin{aligned} T_{\lambda_i\lambda_j\lambda_+\lambda_-}^P(\gamma) &= -e^2\Delta(\gamma)\delta_{ij}[\bar{v}(p_{\mu^+}, \lambda_+)\gamma^\nu u(p_{\mu^-}, \lambda_-)] \\ &\quad \times [\bar{u}(p_{\chi_j^+}, \lambda_j)\gamma_\nu v(p_{\chi_i^-}, \lambda_i)], \end{aligned} \quad (\text{C.29})$$

$$\begin{aligned} T_{\lambda_i\lambda_j\lambda_+\lambda_-}^P(Z) &= -\frac{g^2}{\cos^2 \theta_W}\Delta(Z)[\bar{v}(p_{\mu^+}, \lambda_+)\gamma^\nu(L_\mu P_L + R_\mu P_R)u(p_{\mu^-}, \lambda_-)] \\ &\quad \times [\bar{u}(p_{\chi_j^+}, \lambda_j)\gamma_\nu(O'_{ji}{}^L P_L + O'_{ji}{}^R P_R)v(p_{\chi_i^-}, \lambda_i)], \end{aligned} \quad (\text{C.30})$$

$$\begin{aligned} T_{\lambda_i\lambda_j\lambda_+\lambda_-}^P(\tilde{\nu}) &= -g^2V_{j1}V_{i1}^*\Delta(\tilde{\nu})[\bar{v}(p_{\mu^+}, \lambda_+)P_R v(p_{\chi_j^+}, \lambda_j)] \\ &\quad \times [\bar{u}(p_{\chi_i^-}, \lambda_i)P_L u(p_{\mu^-}, \lambda_-)], \end{aligned} \quad (\text{C.31})$$

with the propagators

$$\Delta(\gamma) = \frac{i}{s}, \quad \Delta(Z) = \frac{i}{s - m_Z^2}, \quad \Delta(\tilde{\nu}) = \frac{i}{t - m_{\tilde{\nu}}^2}, \quad (\text{C.32})$$

and $s = (p_{\mu^+} + p_{\mu^-})^2$, $t = (p_{\mu^+} - p_{\chi_j^+})^2$. We neglect the Z -width in the propagator $\Delta(Z)$ for energies beyond the resonance. The Feynman diagrams are shown in Fig. 2. For e^+e^- collisions, the amplitudes are given in Ref. [51, 52].

The continuum contributions P_{cont} are those from the non-resonant γ , Z and $\tilde{\nu}_\mu$ exchange channels. The coefficient P_{cont} is independent of the chargino polarization. It can be decomposed into contributions from the different continuum channels

$$P_{\text{cont}} = P(\gamma\gamma) + P(\gamma Z) + P(\gamma\tilde{\nu}) + P(ZZ) + P(Z\tilde{\nu}) + P(\tilde{\nu}\tilde{\nu}) \quad (\text{C.33})$$

with

$$P(\gamma\gamma) = \delta_{ij}4e^4|\Delta(\gamma)|^2(c_L + c_R)E_b^2(E_{\chi_j^+}E_{\chi_i^-} + m_{\chi_j^+}m_{\chi_i^-} + q^2\cos^2 \theta), \quad (\text{C.34})$$

$$\begin{aligned} P(\gamma Z) &= \delta_{ij}4\frac{e^2g^2}{\cos^2 \theta_W}E_b^2\Delta(\gamma)\Delta(Z)^*\text{Re}\left\{(L_\mu c_L - R_\mu c_R)(O'_{ij}{}^{R*} - O'_{ij}{}^{L*})2E_b q \cos \theta \right. \\ &\quad \left. + (L_\mu c_L + R_\mu c_R)(O'_{ij}{}^{L*} + O'_{ij}{}^{R*})(E_{\chi_j^+}E_{\chi_i^-} + m_{\chi_j^+}m_{\chi_i^-} + q^2\cos^2 \theta)\right\}, \end{aligned} \quad (\text{C.35})$$

$$P(\gamma\tilde{\nu}) = 2\delta_{ij}e^2g^2E_b^2c_L\Delta(\gamma)\Delta(\tilde{\nu})^*\text{Re}\left\{V_{i1}^*V_{j1}\right\} \\ \times (E_{\chi_j^+}E_{\chi_i^-} + m_{\chi_j^+}m_{\chi_i^-} - 2E_bq\cos\theta + q^2\cos^2\theta), \quad (\text{C.36})$$

$$P(ZZ) = \frac{2g^4}{\cos^4\theta_W}|\Delta(Z)|^2E_b^2\left[(L_\mu^2c_L - R_\mu^2c_R)(|O_{ij}'^R|^2 - |O_{ij}'^L|^2)2E_bq\cos\theta \right. \\ \left. + (L_\mu^2c_L + R_\mu^2c_R)(|O_{ij}'^L|^2 + |O_{ij}'^R|^2)(E_{\chi_j^+}E_{\chi_i^-} + q^2\cos^2\theta) \right. \\ \left. + (L_\mu^2c_L + R_\mu^2c_R)2\text{Re}\{O_{ij}'^L O_{ij}'^{R*}\}m_{\chi_j^+}m_{\chi_i^-}\right], \quad (\text{C.37})$$

$$P(Z\tilde{\nu}) = \frac{2g^4}{\cos^2\theta_W}L_\mu c_L E_b^2\Delta(Z)\Delta(\tilde{\nu})^*\text{Re}\left\{V_{i1}^*V_{j1}\right. \\ \left.\times [O_{ij}'^L(E_{\chi_j^+}E_{\chi_i^-} - 2E_bq\cos\theta + q^2\cos^2\theta) + O_{ij}'^R m_{\chi_j^+}m_{\chi_i^-}]\right\}, \quad (\text{C.38})$$

$$P(\tilde{\nu}\tilde{\nu}) = \frac{g^4}{2}c_L|V_{i1}|^2|V_{j1}|^2|\Delta(\tilde{\nu})|^2E_b^2(E_{\chi_j^+}E_{\chi_i^-} - 2E_bq\cos\theta + q^2\cos^2\theta), \quad (\text{C.39})$$

with the scattering angle $\theta\angle(\vec{p}_{\mu^-}, p_{\tilde{\chi}_i^-})$. The longitudinal beam polarizations are included in the weighting factors

$$c_L = (1 - \mathcal{P}_-)(1 + \mathcal{P}_+), \quad c_R = (1 + \mathcal{P}_-)(1 - \mathcal{P}_+). \quad (\text{C.40})$$

For equal beam polarizations $\mathcal{P}_+ = \mathcal{P}_- \equiv \mathcal{P}$, we thus have $P_{\text{cont}}(\mathcal{P}) = P_{\text{cont}}(-\mathcal{P})$. For e^+e^- collisions, the terms for P_{cont} in the laboratory system are also given in Refs. [52, 53], however they differ by a factor of 2 in our notation (15). Note that the term P_{cont} is invariant under $i \leftrightarrow j$ exchange at tree level if CP is conserved.

The continuum contributions Σ_{cont}^3 (16) to the longitudinal $\tilde{\chi}_j^+$ polarization for chargino production $\mu^+\mu^- \rightarrow \tilde{\chi}_i^-\tilde{\chi}_j^+$ decompose into

$$\Sigma_{\text{cont}}^3 = \Sigma_P^3(\gamma\gamma) + \Sigma_P^3(\gamma Z) + \Sigma_P^3(\gamma\tilde{\nu}) + \Sigma_P^3(ZZ) + \Sigma_P^3(Z\tilde{\nu}) + \Sigma_P^3(\tilde{\nu}\tilde{\nu}), \quad (\text{C.41})$$

with

$$\Sigma_P^3(\gamma\gamma) = \delta_{ij}4e^4|\Delta(\gamma)|^2(c_L - c_R)E_b^2\cos\theta(q^2 + E_{\chi_j^+}E_{\chi_i^-} + m_{\chi_j^+}m_{\chi_i^-}), \quad (\text{C.42})$$

$$\Sigma_P^3(\gamma Z) = \delta_{ij}4\frac{e^2g^2}{\cos^2\theta_W}E_b^2\Delta(\gamma)\Delta(Z)^* \\ \times \text{Re}\left\{(L_\mu c_L - R_\mu c_R)(O_{ji}'^{R*} + O_{ji}'^{L*})(q^2 + E_{\chi_j^+}E_{\chi_i^-} + m_{\chi_j^+}m_{\chi_i^-})\cos\theta \right. \\ \left. + (L_\mu c_L + R_\mu c_R)(O_{ji}'^{R*} - O_{ji}'^{L*})q(E_{\chi_i^-} + E_{\chi_j^+}\cos^2\theta)\right\}, \quad (\text{C.43})$$

$$\Sigma_P^3(\gamma\tilde{\nu}) = -\delta_{ij}2e^2g^2c_LE_b^2\Delta(\gamma)\Delta(\tilde{\nu})^*\text{Re}\left\{V_{j1}^*V_{i1}\right\} \\ \times [qE_{\chi_i^-} - (q^2 + E_{\chi_j^+}E_{\chi_i^-})\cos\theta + qE_{\chi_j^+}\cos^2\theta - m_{\chi_j^+}m_{\chi_i^-}\cos\theta], \quad (\text{C.44})$$

$$\Sigma_P^3(ZZ) = \frac{2g^4}{\cos^4\theta_W}|\Delta(Z)|^2E_b^2\left[(L_\mu^2c_L + R_\mu^2c_R)(|O_{ji}'^R|^2 - |O_{ji}'^L|^2)q(E_{\chi_i^-} + E_{\chi_j^+}\cos^2\theta) \right. \\ \left. + (L_\mu^2c_L - R_\mu^2c_R)2\text{Re}\{O_{ji}'^L O_{ji}'^{R*}\}m_{\chi_j^+}m_{\chi_i^-}\cos\theta \right. \\ \left. + (L_\mu^2c_L - R_\mu^2c_R)(|O_{ji}'^L|^2 + |O_{ji}'^R|^2)(q^2 + E_{\chi_j^+}E_{\chi_i^-})\cos\theta\right], \quad (\text{C.45})$$

$$\begin{aligned}\Sigma_P^3(Z\tilde{\nu}) &= \frac{2g^4}{\cos^2\theta_W} L_\mu c_L E_b^2 \Delta(Z) \Delta(\tilde{\nu})^* \text{Re} \left\{ V_{j1}^* V_{i1} [O_{ji}'^R m_{\chi_j^+} m_{\chi_i^-} \cos\theta \right. \\ &\quad \left. - O_{ji}'^L (qE_{\chi_i^-} - (q^2 + E_{\chi_j^+} E_{\chi_i^-}) \cos\theta + qE_{\chi_j^+} \cos^2\theta) \right\},\end{aligned}\quad (\text{C.46})$$

$$\begin{aligned}\Sigma_P^3(\tilde{\nu}\tilde{\nu}) &= -\frac{g^4}{2} c_L |V_{j1}|^2 |V_{i1}|^2 |\Delta(\tilde{\nu})|^2 E_b^2 \\ &\quad \times [qE_{\chi_i^-} - (q^2 + E_{\chi_j^+} E_{\chi_i^-}) \cos\theta + qE_{\chi_j^+} \cos^2\theta].\end{aligned}\quad (\text{C.47})$$

For e^+e^- collisions, the terms for Σ_{cont}^3 for chargino $\tilde{\chi}_j^+$ in the laboratory system are also given in Ref. [52, 53], however they differ by a factor of 2 in our notation (15). In order to obtain the corresponding polarization terms for the other chargino $\tilde{\chi}_i^-$, one has to substitute $E_{\chi_j^+} \leftrightarrow E_{\chi_i^-}$ and $m_{\chi_j^+} \leftrightarrow m_{\chi_i^-}$ in Eqs. (C.42)-(C.47); in addition, one has to change the overall sign [52]. Note that for the charge conjugated process $\mu^+\mu^- \rightarrow \tilde{\chi}_i^+ \tilde{\chi}_j^-$, the averaged chargino $\tilde{\chi}_j^\pm$ polarization of the continuum, see Eq. (26), changes sign, i.e., $\bar{\Sigma}_{\text{cont}}^3(\tilde{\chi}_i^+ \tilde{\chi}_j^-) = -\bar{\Sigma}_{\text{cont}}^3(\tilde{\chi}_i^- \tilde{\chi}_j^+)$. For equal beam polarizations $\mathcal{P}_+ = \mathcal{P}_- \equiv \mathcal{P}$, the terms obey $\Sigma_{\text{cont}}^3(-\mathcal{P}) = \Sigma_{\text{cont}}^3(\mathcal{P})$, see Eq. (C.40).

D Chargino decay into leptons and W boson

The expansion coefficients of the chargino decay matrix (A.9) for the chargino decay $\tilde{\chi}_j^+ \rightarrow \ell^+ \tilde{\nu}_\ell$, with $\ell = e, \mu$, are

$$D = \frac{g^2}{2} |V_{j1}|^2 (m_{\chi_j^\pm}^2 - m_{\tilde{\nu}_\ell}^2), \quad (\text{D.48})$$

$$\Sigma_D^a = -g^2 |V_{j1}|^2 m_{\chi_j^\pm} (s_{\chi_j^\pm}^a \cdot p_\ell). \quad (\text{D.49})$$

The coefficient Σ_D^a for the charge conjugated process, $\tilde{\chi}_j^- \rightarrow \ell^- \tilde{\nu}_\ell^*$, is obtained by inverting the sign of Eq. (D.49). With these definitions, we can rewrite the factor Σ_D^3 , that multiplies the longitudinal chargino polarization Σ_P^3 in Eq. (15),

$$\Sigma_D^3 = \eta_{\ell\pm} \frac{D}{\Delta_\ell} (E_\ell - \hat{E}_\ell), \quad (\text{D.50})$$

where we have used

$$m_{\chi_j^\pm} (s_{\chi_j^\pm}^3 \cdot p_\ell) = -\frac{m_{\chi_j^\pm}^2}{|\vec{p}_{\chi_j^\pm}|} (E_\ell - \hat{E}_\ell). \quad (\text{D.51})$$

Similar results can be obtained for the chargino decay into a τ , $\tilde{\chi}_j^\pm \rightarrow \tau^\pm \tilde{\nu}_\tau^{(*)}$, and W boson, $\tilde{\chi}_j^\pm \rightarrow W^\pm \tilde{\chi}_k^0$ [33]. The corresponding interaction Lagrangians are [1]

$$\mathcal{L}_{\tau\tilde{\nu}_\tau\tilde{\chi}^+} = -g\bar{\tau}(V_{j1}P_R - Y_\tau U_{j2}^*P_L)\tilde{\chi}_j^{+C}\tilde{\nu}_\tau + \text{h.c.}, \quad (\text{D.52})$$

$$\mathcal{L}_{W^-\tilde{\chi}^+\tilde{\chi}^0} = gW_\mu^-\tilde{\chi}_k^0\gamma^\mu(O_{kj}^LP_L + O_{kj}^RP_R)\tilde{\chi}_j^+\tilde{\nu}_\ell + \text{h.c.}, \quad (\text{D.53})$$

respectively, with the couplings

$$O_{kj}^L = -\frac{1}{\sqrt{2}}N_{k4}V_{j2}^* + (\sin\theta_W N_{k1} + \cos\theta_W N_{k2})V_{j1}^*, \quad (\text{D.54})$$

$$O_{kj}^R = +\frac{1}{\sqrt{2}}N_{k3}^*U_{j2} + (\sin\theta_W N_{k1}^* + \cos\theta_W N_{k2}^*)U_{j1}, \quad (\text{D.55})$$

and $Y_\tau = m_\tau/(\sqrt{2}m_W \cos\beta)$. The 4×4 unitary matrix N diagonalizes the neutralino mass matrix Y in the basis $\{\tilde{\gamma}, \tilde{Z}, \tilde{h}_1, \tilde{h}_2\}$ with $N_{il}^* Y_{lm} N_{mj}^\dagger = \delta_{ij} m_{\chi_j^0}$ [1].

The expansion coefficients of the chargino decay matrix (A.9) for $\tilde{\chi}_j^+ \rightarrow \tau^+ \tilde{\nu}_\tau$ are

$$D = \frac{g^2}{2}(|V_{j1}|^2 + Y_\tau^2 |U_{j2}|^2)(m_{\chi_j^\pm}^2 - m_{\tilde{\nu}_\tau}^2), \quad (\text{D.56})$$

$$\Sigma_D^a = -g^2(|V_{j1}|^2 - Y_\tau^2 |U_{j2}|^2)m_{\chi_j^\pm}(s_{\chi_j^\pm}^a \cdot p_\tau), \quad (\text{D.57})$$

and those for $\tilde{\chi}_j^+ \rightarrow W^+ \tilde{\chi}_k^0$ are

$$D = \frac{g^2}{2}(|O_{kj}^L|^2 + |O_{kj}^R|^2) \left[m_{\chi_j^\pm}^2 + m_{\chi_k^0}^2 - 2m_W^2 + \frac{(m_{\chi_j^\pm}^2 - m_{\chi_k^0}^2)^2}{m_W^2} \right] - 6g^2 \text{Re}(O_{kj}^L O_{kj}^{R*}) m_{\chi_j^\pm} m_{\chi_k^0}, \quad (\text{D.58})$$

$$\Sigma_D^a = -g^2(|O_{kj}^L|^2 - |O_{kj}^R|^2) \frac{(m_{\chi_j^\pm}^2 - m_{\chi_k^0}^2 - 2m_W^2)}{m_W^2} m_{\chi_j^\pm}(s_{\chi_j^\pm}^a \cdot p_W). \quad (\text{D.59})$$

The coefficients Σ_D^a for the charge conjugated processes, $\tilde{\chi}_j^- \rightarrow \tau^- \tilde{\nu}_\tau^*$ and $\tilde{\chi}_j^- \rightarrow W^- \tilde{\chi}_k^0$, are obtained by inverting the signs of Eqs. (D.57) and (D.59), respectively.

For the chargino decay $\tilde{\chi}_j^\pm \rightarrow W^\pm \tilde{\chi}_k^0$, the energy limits of the W boson are $E_W^{\text{max(min)}} = \hat{E}_W \pm \Delta_W$, see Eq. (21), with

$$\hat{E}_W = \frac{E_W^{\text{max}} + E_W^{\text{min}}}{2} = \frac{m_{\chi_j^\pm}^2 + m_W^2 - m_{\chi_k^0}^2}{2m_{\chi_j^\pm}^2} E_{\chi_j^\pm}, \quad (\text{D.60})$$

$$\Delta_W = \frac{E_W^{\text{max}} - E_W^{\text{min}}}{2} = \frac{\sqrt{\lambda(m_{\chi_j^\pm}^2, m_W^2, m_{\chi_k^0}^2)}}{2m_{\chi_j^\pm}^2} |\vec{p}_{\chi_j^\pm}|. \quad (\text{D.61})$$

The decay factor (24) is

$$\eta_{W^\pm} = \pm \frac{(|O_{kj}^L|^2 - |O_{kj}^R|^2)f_1}{(|O_{kj}^L|^2 + |O_{kj}^R|^2)f_2 + \text{Re}\{O_{kj}^L O_{kj}^{R*}\}f_3}, \quad (\text{D.62})$$

with

$$\begin{aligned} f_1 &= (m_{\chi_j^\pm}^2 - m_{\chi_k^0}^2 - 2m_W^2) \sqrt{\lambda(m_{\chi_j^\pm}^2, m_W^2, m_{\chi_k^0}^2)}, \\ f_2 &= (m_{\chi_j^\pm}^2 + m_{\chi_k^0}^2 - 2m_W^2) m_W^2 + (m_{\chi_j^\pm}^2 - m_{\chi_k^0}^2)^2, \\ f_3 &= -12 m_{\chi_j^\pm} m_{\chi_k^0} m_W^2. \end{aligned}$$

For the chargino decay $\tilde{\chi}_j^\pm \rightarrow \tau^\pm \tilde{\nu}_\tau^{(*)}$, the decay factor (24) is obtained from Eqs. (D.56) and (D.57)

$$\eta_{\tau^\pm} = \pm \frac{|V_{j1}|^2 - Y_\tau^2 |U_{j2}|^2}{|V_{j1}|^2 + Y_\tau^2 |U_{j2}|^2}. \quad (\text{D.63})$$

The coefficients η_{W^\pm} , and also η_{τ^\pm} (D.63), depend on the chargino couplings, as well as on the chargino and neutralino masses, which could be measured at the international linear collider (ILC) with high precision [54, 55].

In order to reduce the free MSSM parameters, we parametrize the slepton masses with their approximate renormalization group equations (RGE) [61]

$$m_{\tilde{\ell}_R}^2 = m_0^2 + m_\ell^2 + 0.23 M_2^2 - m_Z^2 \cos 2\beta \sin^2 \theta_W, \quad (\text{D.64})$$

$$m_{\tilde{\ell}_L}^2 = m_0^2 + m_\ell^2 + 0.79 M_2^2 + m_Z^2 \cos 2\beta \left(-\frac{1}{2} + \sin^2 \theta_W\right), \quad (\text{D.65})$$

$$m_{\tilde{\nu}_\ell}^2 = m_0^2 + m_\ell^2 + 0.79 M_2^2 + \frac{1}{2} m_Z^2 \cos 2\beta, \quad (\text{D.66})$$

with m_0 the common scalar mass parameter the GUT scale.

E Cross sections

We obtain cross sections and distributions by integrating the amplitude squared $|T|^2$ (15) over the Lorentz invariant phase space element $d\text{Lips}$

$$d\sigma = \frac{1}{2s} |T|^2 d\text{Lips}. \quad (\text{E.67})$$

We use the narrow width approximation for the propagator of the decaying chargino. The approximation is justified for $\Gamma_{\chi_j}/m_{\chi_j} \ll 1$, which holds in our case with $\Gamma_{\chi_j} \lesssim \mathcal{O}(1\text{GeV})$. Note, however, that the naive $\mathcal{O}(\Gamma/m)$ -expectation of the error can easily receive large off-shell corrections of an order of magnitude and more, in particular at threshold or due to interferences with other resonant or non-resonant processes. For a recent discussion of these issues, see [62, 63]

Explicit formulas of the phase space for chargino production (1) and decay (2), can be found, e.g., in Ref. [53]. The cross section for chargino production is

$$\sigma_{ij} = \frac{\sqrt{\lambda_{ij}}}{8\pi s^2} \bar{P}, \quad (\text{E.68})$$

with the triangle function λ_{ij} (A.13), and \bar{P} given in Eq. (26). The integrated cross section for chargino production (1) and subsequent leptonic decay $\tilde{\chi}_j^+ \rightarrow \ell^+ \tilde{\nu}_\ell$ (2) is given by

$$\sigma_{ij,\ell} = \frac{1}{64\pi^2} \frac{\sqrt{\lambda_{ij}}}{s^2} \frac{(m_{\chi_j^+}^2 - m_{\tilde{\nu}_\ell}^2)}{m_{\chi_j^+}^3 \Gamma_{\chi_j^+}} \bar{P} D = \sigma_{ij} \times \text{BR}(\tilde{\chi}_j^+ \rightarrow \ell^+ \tilde{\nu}_\ell). \quad (\text{E.69})$$

The integrated cross section for chargino production and subsequent decay $\tilde{\chi}_j^+ \rightarrow W^+ \tilde{\chi}_k^0$ (3) is

$$\sigma_{ij,W} = \frac{1}{64\pi^2} \frac{\sqrt{\lambda_{ij}}}{s^2} \frac{\sqrt{\lambda(m_{\tilde{\chi}_j^+}^2, m_{\tilde{\chi}_k^0}^2, m_W^2)}}{m_{\tilde{\chi}_j^+}^3 \Gamma_{\tilde{\chi}_j^+}} \bar{P}D = \sigma_{ij} \times \text{BR}(\tilde{\chi}_j^+ \rightarrow W^+ \tilde{\chi}_k^0). \quad (\text{E.70})$$

F Statistical significances

We define the statistical significances of the C-even cross section observable $\mathcal{A}_{ij}^{\text{C+P-}}$ (30) by [7]

$$\mathcal{S}_{ij}^{\text{C+P-}} = |\mathcal{A}_{ij}^{\text{C+P-}}| \sqrt{2(2 - \delta_{ij}) \sigma_{ij}^{\text{C+P+}} \mathcal{L}}, \quad (\text{F.71})$$

where \mathcal{L} denotes the integrated luminosity for chargino production, and $\sigma_{ij}^{\text{C+P+}}$ is the C and P symmetrized chargino production cross section, defined in Eq. (28). There is a factor 2 appearing in Eq. (F.71), since the asymmetries require two sets of equal beam polarizations $\pm \mathcal{P}$. There is a factor $(2 - \delta_{ij})$, since two independent cross section measurements are available for $i \neq j$, but only one for $i = j$. The significances for the C-odd asymmetries $\mathcal{A}_{ij}^{\text{C-P}\pm}$, Eqs. (31), and (32), are defined by

$$\mathcal{S}_{ij}^{\text{C-P}\pm} = |\mathcal{A}_{ij}^{\text{C-P}\pm}| \sqrt{4 \sigma_{ij}^{\text{C+P+}} \mathcal{L}}. \quad (\text{F.72})$$

Note that the C-odd production asymmetries $\mathcal{A}_{ij}^{\text{C-P}\pm}$ vanish trivially for $i = j$.

The significances for the CP-odd decay asymmetries $\mathcal{A}_{ij,\lambda}^{\text{C}\pm\text{P}\mp}$, Eqs. (38) and (40), are defined by [7]

$$\mathcal{S}_{ij,\lambda}^{\text{C}\pm\text{P}\mp} = |\mathcal{A}_{ij,\lambda}^{\text{C}\pm\text{P}\mp}| \sqrt{4 \sigma_{ij}^{\text{C+P+}} \text{BR}(\tilde{\chi}_j^+ \rightarrow \lambda^+ \tilde{N}_\lambda) \mathcal{L}_{\text{eff}}}, \quad (\text{F.73})$$

and similarly for the CP-even asymmetries $\mathcal{A}_{ij,\lambda}^{\text{C}\pm\text{P}\pm}$, Eqs. (38) and (42),

$$\mathcal{S}_{ij,\lambda}^{\text{C}\pm\text{P}\pm} = |\mathcal{A}_{ij,\lambda}^{\text{C}\pm\text{P}\pm}| \sqrt{4 \sigma_{ij}^{\text{C+P+}} \text{BR}(\tilde{\chi}_j^+ \rightarrow \lambda^+ \tilde{N}_\lambda) \mathcal{L}_{\text{eff}}}, \quad (\text{F.74})$$

with $\lambda = \ell$ or W , and \tilde{N}_λ the associated sneutrino or neutralino, respectively. The effective integrated luminosity is $\mathcal{L}_{\text{eff}} = \epsilon_\lambda \mathcal{L}$, with the detection efficiency ϵ_λ of the leptons or W bosons in the chargino decay $\tilde{\chi}_j^\pm \rightarrow \ell^\pm \tilde{\nu}_\ell^{(*)}$ or $\tilde{\chi}_j^\pm \rightarrow W^\pm \tilde{\chi}_k^0$, respectively. There is a factor 4 appearing in the significances, Eqs. (F.73) and (F.74), since the asymmetries require two sets of equal beam polarizations $\pm \mathcal{P}$, as well as two decay modes, $\tilde{\chi}_j^+ \rightarrow \lambda^+ \tilde{N}_\lambda$ and the charge conjugated decay $\tilde{\chi}_j^- \rightarrow \lambda^- \tilde{N}_\lambda^{(*)}$.

For an ideal detector a significance of, e.g., $\mathcal{S} = 1$ implies that the asymmetries can be measured at the statistical 68% confidence level. In order to predict the absolute values of confidence levels, clearly detailed Monte Carlo analysis including detector and background simulations with particle identification and reconstruction efficiencies would be required, which is however beyond the scope of the present work.

References

- [1] H. Haber, K. Kane, Phys. Rep. **117** (1985) 75.
- [2] J. F. Gunion and H. E. Haber, Nucl. Phys. B **272**, 1 (1986) [Erratum-ibid. B **402**, 567 (1993)].
- [3] J. F. Gunion, H. E. Haber, G. L. Kane and S. Dawson, “*The Higgs Hunter’s Guide*” (Addison-Wesley Publishing Company, Redwood City, CA, USA, 1990).
- [4] M. S. Carena and H. E. Haber, Prog. Part. Nucl. Phys. **50**, 63 (2003) [arXiv:hep-ph/0208209].
- [5] A. Djouadi, arXiv:hep-ph/0503173.
- [6] E. Accomando *et al.*, arXiv:hep-ph/0608079.
- [7] H. Fraas, O. Kittel and F. von der Pahlen, “*Higgs boson interference in chargino and neutralino production at the muon collider*”, in Ref. [6], p. 169.
- [8] A. Pilaftsis, Nucl. Phys. B **504** (1997) 61 [arXiv:hep-ph/9702393].
- [9] A. Pilaftsis, Phys. Rev. D **58**, 096010 (1998) [arXiv:hep-ph/9803297]; Phys. Lett. B **435**, 88 (1998) [arXiv:hep-ph/9805373].
- [10] J. F. Gunion, B. Grzadkowski, H. E. Haber and J. Kalinowski, Phys. Rev. Lett. **79** (1997) 982 [arXiv:hep-ph/9704410];
B. Grzadkowski, J. F. Gunion and J. Kalinowski, Phys. Rev. D **60** (1999) 075011 [arXiv:hep-ph/9902308].
- [11] D. A. Demir, Phys. Rev. D **60** (1999) 055006 [arXiv:hep-ph/9901389];
S. Y. Choi, M. Drees and J. S. Lee, Phys. Lett. B **481** (2000) 57 [arXiv:hep-ph/0002287];
G. L. Kane and L. T. Wang, Phys. Lett. B **488** (2000) 383 [arXiv:hep-ph/0003198];
T. Ibrahim and P. Nath, Phys. Rev. D **63**, 035009 (2001) [arXiv:hep-ph/0008237];
Phys. Rev. D **64** (2001) 035009 [arXiv:hep-ph/0102218];
Phys. Rev. D **66**, 015005 (2002) [arXiv:hep-ph/0204092];
S. W. Ham, S. K. Oh, E. J. Yoo, C. M. Kim and D. Son, Phys. Rev. D **68** (2003) 055003 [arXiv:hep-ph/0205244].
- [12] A. Pilaftsis and C. E. M. Wagner, Nucl. Phys. B **553** (1999) 3 [arXiv:hep-ph/9902371];
M. S. Carena, J. R. Ellis, A. Pilaftsis and C. E. M. Wagner, Nucl. Phys. B **586** (2000) 92 [arXiv:hep-ph/0003180];
M. S. Carena, J. R. Ellis, A. Pilaftsis and C. E. M. Wagner, Nucl. Phys. B **625**, 345 (2002) [arXiv:hep-ph/0111245].

- [13] S. Y. Choi, J. Kalinowski, Y. Liao and P. M. Zerwas, Eur. Phys. J. C **40** (2005) 555 [arXiv:hep-ph/0407347].
- [14] S. Heinemeyer, Eur. Phys. J. C **22** (2001) 521 [arXiv:hep-ph/0108059].
- [15] S. Heinemeyer, W. Hollik, H. Rzehak and G. Weiglein, arXiv:0705.0746 [hep-ph].
- [16] M. Frank, T. Hahn, S. Heinemeyer, W. Hollik, H. Rzehak and G. Weiglein, JHEP **0702** (2007) 047 [arXiv:hep-ph/0611326].
- [17] G. Degrandi, S. Heinemeyer, W. Hollik, P. Slavich and G. Weiglein, Eur. Phys. J. C **28** (2003) 133 [arXiv:hep-ph/0212020];
S. Heinemeyer, W. Hollik and G. Weiglein, Eur. Phys. J. C **9** (1999) 343 [arXiv:hep-ph/9812472]; Comput. Phys. Commun. **124** (2000) 76 [arXiv:hep-ph/9812320].
- [18] J. S. Lee, A. Pilaftsis, M. S. Carena, S. Y. Choi, M. Drees, J. R. Ellis and C. E. M. Wagner, Comput. Phys. Commun. **156**, 283 (2004) [arXiv:hep-ph/0307377];
J. S. Lee, M. Carena, J. Ellis, A. Pilaftsis and C. E. M. Wagner, arXiv:0712.2360 [hep-ph].
- [19] M. Carena, J. R. Ellis, A. Pilaftsis and C. E. M. Wagner, Phys. Lett. B **495** (2000) 155 [arXiv:hep-ph/0009212].
- [20] R. Barate *et al.* [LEP Working Group for Higgs boson searches], Phys. Lett. B **565**, 61 (2003) [arXiv:hep-ex/0306033];
S. Schael *et al.* [ALEPH Collaboration], Eur. Phys. J. C **47**, 547 (2006) [arXiv:hep-ex/0602042];
P. Bandyopadhyay, A. Datta, A. Datta and B. Mukhopadhyaya, arXiv:0710.3016 [hep-ph];
A. Belyaev, Q. H. Cao, D. Nomura, K. Tobe and C. P. Yuan, Phys. Rev. Lett. **100**, 061801 (2008) [arXiv:hep-ph/0609079].
- [21] K. E. Williams and G. Weiglein, Phys. Lett. B **660** (2008) 217 [arXiv:0710.5320 [hep-ph]]; arXiv:0710.5331 [hep-ph].
- [22] S. Berge, W. Bernreuther and J. Ziethe, Phys. Rev. Lett. **100**, 171605 (2008) [arXiv:0801.2297 [hep-ph]];
R. M. Godbole, D. J. Miller and M. M. Muhlleitner, JHEP **0712**, 031 (2007) [arXiv:0708.0458 [hep-ph]];
P. S. Bhupal Dev, A. Djouadi, R. M. Godbole, M. M. Muhlleitner and S. D. Rindani, Phys. Rev. Lett. **100**, 051801 (2008) [arXiv:0707.2878 [hep-ph]];
S. Hesselbach, S. Moretti, S. Munir and P. Poulose, Eur. Phys. J. C **54**, 129 (2008) [arXiv:0706.4269 [hep-ph]].
- [23] A. Dobado, M. J. Herrero and S. Penaranda, Eur. Phys. J. C **17**, 487 (2000) [arXiv:hep-ph/0002134];

- J. F. Gunion and H. E. Haber, Phys. Rev. D **67**, 075019 (2003) [arXiv:hep-ph/0207010];
H. E. Haber and Y. Nir, Phys. Lett. B **306**, 327 (1993) [arXiv:hep-ph/9302228];
H. E. Haber, arXiv:hep-ph/9505240.
- [24] J. R. Ellis, J. S. Lee and A. Pilaftsis, Phys. Rev. D **70**, 075010 (2004) [arXiv:hep-ph/0404167]; Phys. Rev. D **72**, 095006 (2005) [arXiv:hep-ph/0507046].
- [25] B. Grzadkowski and J. F. Gunion, Phys. Lett. B **350**, 218 (1995) [arXiv:hep-ph/9501339].
- [26] V. D. Barger, M. S. Berger, J. F. Gunion and T. Han, Phys. Rept. **286** (1997) 1 [arXiv:hep-ph/9602415];
R. Casalbuoni, A. Deandrea, S. De Curtis, D. Dominici, R. Gatto and J. F. Gunion, JHEP **9908** (1999) 011 [arXiv:hep-ph/9904268];
M. S. Berger, Phys. Rev. Lett. **87**, 131801 (2001) [arXiv:hep-ph/0105128].
- [27] S. Dittmaier and A. Kaiser, Phys. Rev. D **65**, 113003 (2002) [arXiv:hep-ph/0203120].
- [28] H. Fraas, F. Franke, G. Moortgat-Pick, F. von der Pahlen and A. Wagner, Eur. Phys. J. C **29** (2003) 587 [arXiv:hep-ph/0303044].
- [29] B. Grzadkowski, J. F. Gunion and J. Pliszka, Nucl. Phys. B **583**, 49 (2000) [arXiv:hep-ph/0003091].
- [30] E. Asakawa, A. Sugamoto and I. Watanabe, Eur. Phys. J. C **17**, 279 (2000).
- [31] V. D. Barger, T. Han and C. G. Zhou, Phys. Lett. B **480**, 140 (2000) [arXiv:hep-ph/0002042].
- [32] H. Fraas, F. von der Pahlen and C. Sachse, Eur. Phys. J. **C37** (2004) 495 [arXiv:hep-ph/0407057].
- [33] O. Kittel and F. von der Pahlen, Phys. Rev. D **72** (2005) 095004 [arXiv:hep-ph/0508267].
- [34] E. Asakawa, S. Y. Choi and J. S. Lee, Phys. Rev. D **63** (2001) 015012 [arXiv:hep-ph/0005118].
- [35] D. Atwood and A. Soni, Phys. Rev. D **52**, 6271 (1995) [arXiv:hep-ph/9505233].
- [36] A. Pilaftsis, Phys. Rev. Lett. **77** (1996) 4996 [arXiv:hep-ph/9603328].
- [37] K. S. Babu, C. F. Kolda, J. March-Russell and F. Wilczek, Phys. Rev. D **59** (1999) 016004 [arXiv:hep-ph/9804355].
- [38] S. Y. Choi and J. S. Lee, Phys. Rev. D **61** (2000) 111702 [arXiv:hep-ph/9909315].

- [39] S. Y. Choi, M. Drees, B. Gaissmaier and J. S. Lee, Phys. Rev. D **64** (2001) 095009 [arXiv:hep-ph/0103284].
- [40] J. Bernabeu, D. Binosi and J. Papavassiliou, JHEP **0609**, 023 (2006) [arXiv:hep-ph/0604046].
- [41] Z. Hioki, T. Konishi and K. Ohkuma, JHEP **0707**, 082 (2007) [arXiv:0706.4346 [hep-ph]].
- [42] H. K. Dreiner, O. Kittel and F. von der Pahlen, JHEP **0801** (2008) 017 [arXiv:0711.2253 [hep-ph]].
- [43] V. D. Barger, M. S. Berger, J. F. Gunion and T. Han, Nucl. Phys. Proc. Suppl. **51A** (1996) 13 [arXiv:hep-ph/9604334].
- [44] Proceedings of *Prospective Study of Muon Storage Rings at CERN*, Eds. B. Autin, A. Blondel, J. Ellis, CERN yellow report, CERN 99-02, ECFA 99-197, April 30 (1999);
V. D. Barger, M. Berger, J. F. Gunion and T. Han, *In the Proceedings of APS / DPF / DPB Summer Study on the Future of Particle Physics (Snowmass 2001), Snowmass, Colorado, 30 Jun - 21 Jul 2001, pp E110* [arXiv:hep-ph/0110340];
A. Blondel *et al.*, “*ECFA/CERN studies of a European neutrino factory complex*,” CERN-2004-002.
- [45] C. Blöchliger *et al.*, Higgs working group of the ECFA-CERN study on Neutrino Factory & Muon Storage Rings at CERN, *Physics Opportunities at $\mu^+\mu^-$ Higgs Factories* CERN-TH/2002-028, [arXiv:hep-ph/0202199];
- [46] P. Osland and A. Vereshagin, Phys. Rev. D **76** (2007) 036001 [arXiv:0704.2165 [hep-ph]].
- [47] K. Rolbiecki and J. Kalinowski, arXiv:0709.2994 [hep-ph];
P. Osland, J. Kalinowski, K. Rolbiecki and A. Vereshagin, arXiv:0709.3358 [hep-ph];
K. Rolbiecki and J. Kalinowski, arXiv:0710.3318 [hep-ph].
- [48] J. S. Lee, Mod. Phys. Lett. A **22**, 1191 (2007) [arXiv:0705.1089 [hep-ph]];
R. M. Godbole, S. Kraml, S. D. Rindani and R. K. Singh, Phys. Rev. D **74**, 095006 (2006) [Erratum-ibid. D **74**, 119901 (2006)] [arXiv:hep-ph/0609113];
J. R. Ellis, J. S. Lee and A. Pilaftsis, Nucl. Phys. B **718**, 247 (2005) [arXiv:hep-ph/0411379].
- [49] R.A. Horn, C.A. Johnson, Matrix Analysis, Cambridge University Press 1990.
- [50] H. E. Haber, Proceedings of the 21st SLAC Summer Institute on Particle Physics: *Spin Structure in High Energy Processes*, SLAC, Stanford, CA 1993 [arXiv:hep-ph/9405376].
- [51] G. A. Moortgat-Pick, H. Fraas, A. Bartl and W. Majerotto, Eur. Phys. J. C **7**, 113 (1999) [arXiv:hep-ph/9804306].

- [52] G. Moortgat-Pick, “Spin effects in chargino/neutralino production and decay”, in German, doctoral thesis (1999), University of Würzburg, Germany.
- [53] O. Kittel, arXiv:hep-ph/0504183.
- [54] “TESLA Technical Design Report Part III: *Physics at an $e+e-$ Linear Collider*,” arXiv:hep-ph/0106315.
- [55] A. Djouadi, J. Lykken, K. Monig, Y. Okada, M. J. Oreglia and S. Yamashita, “International Linear Collider Reference Design Report Volume 2: *Physics at the ILC*,” arXiv:0709.1893 [hep-ph].
- [56] W. M. Yao *et al.* [Particle Data Group], J. Phys. G **33** (2006) 1.
- [57] P. G. Harris *et al.*, Phys. Rev. Lett. **82** (1999) 904.
- [58] B. C. Regan, E. D. Commins, C. J. Schmidt and D. DeMille, Phys. Rev. Lett. **88** (2002) 071805.
- [59] M. V. Romalis, W. C. Griffith and E. N. Fortson, Phys. Rev. Lett. **86** (2001) 2505 [arXiv:hep-ex/0012001].
- [60] S. Y. Choi, K. Hagiwara, H. U. Martyn, K. Mawatari and P. M. Zerwas, Eur. Phys. J. C **51**, 753 (2007) [arXiv:hep-ph/0612301].
- [61] L. J. Hall and J. Polchinski, Phys. Lett. B **152** (1985) 335.
- [62] K. Hagiwara *et al.*, Phys. Rev. D **73** (2006) 055005 [arXiv:hep-ph/0512260].
- [63] D. Berdine, N. Kauer and D. Rainwater, Phys. Rev. Lett. **99**, 111601 (2007) [arXiv:hep-ph/0703058];
N. Kauer, Phys. Lett. B **649**, 413 (2007) [arXiv:hep-ph/0703077].